UNIVERSITÀ DEGLI STUDI DI TRENTO
Dipartimento di Ingegneria Civile
e Ambientale

GEOTOP

A Hydrological Balance Model

Technical Description and Programs Guide

Version 0.75

Giacomo Bertoldi
Riccardo Rigon

February 2004

Contents

Chapter 1

Geotop concept and history

a personal view

Riccardo Rigon

The idea to implement and develop GEOTOP is simultaneous to the birth of the project of the Notes on the Fundamentals of Hydrology [Rigon, 2003]. K. Beven describes the mood being at its base very well: " *As scientists we are intrigued by the possibility of assembling our knowledge into a neat package to show that we do, after all, understand our science and its complex interrelated phenomena.* " (W.M., Kohler, 1969).

1.1 GEOTOP$_{0.5}$

(mostly financed by PATT-Serraia project and Cofin 1999)

The very first step was due to the reading of the Entekhaby summary [e.g. - Marani and Rigon (eds), 1997] with the Master thesis of Paolo Verardo and his subsequent work [1998]. We spent together around a year to implement a decent model for evapotranspiration in a complex terrain environment. Actually, most of the time was not spent in implementing the equations of Penman-Monteith, a task easily performed, but in building all the necessary incoming radiation treatments. Especially the view angle and the shadowing routine were delicate to implement. We also faced for the first time the problem of data assimilation and regionalization (at that time the only data we had were those coming from traditional hydro-meteorological stations and we do not have many of them). Apart from the geomorphological data that we extract from DEMs (the "sine qua non" basis of all our work) we had to regionalize: air-surface temperature (varying obviously with the elevation of the terrain), net radiation (that has to be first derived from that at the atmosphere top by the evaluation of an atmospheric thickness which has to be regionalized too) and wind speed. In sequence we decided to use: kriging and a model and the hypothesis of adiabatic temperature profile (for air temperature); Brutsaert [1983] paper results (for atmosphere emissivity) and constant (or kriged) wind speed everywhere. However simplified these solution can appear, they are still at the core of GEOTOP and need to be changed and improved soon. The heat conduction into the ground was parametrized as a linear combination of a sinusoidal function as Entekhaby suggested [1997] (this has been changed). In that work we were also much inspired by the IPW (Image Processing Workbench) [Frew, 1990] routines and we have somehow stolen some ideas from them. Actually we tried to get IPW working for us but its pervasive scripting base (scripting is good but there is a point

after which it makes the code organization unclear), the discontinued support and our ignorance led us to try to builtd a system from the scratch.

In spite of the approximations introduced, our model worked fairly well in estimating the net longwave and shortwave radiation in any point across a basin and at any hour of the day, and could give also reliable estimates of the potential evapotranspiration on a daily basis. However to obtain the real evapotranspiration was a different question. Anyway, our first step in the determination of when and where soil or vegetation humidity availability was enough to sustain the potential evapotranspiration was done by a second Master Thesis by Marco Pegoretti [1999]. He added to the evapotranspiration modules a rainfall-runoff model (temporary called GEOMODEL). Let me say that my approach to the problem of rainfall-runoff has been strongly influenced by the work of Rodriguez-Iturbe and Valdes [1979] and Gupta et al [1980] and I was reluctant to abandon the simplicity of a GIUH-based model in favor of the distributed model. Of the many ideas behind the theory of the GIUH (or GUH as the original authors called it) there is the observation that the river basin is a complex system (an interplay of hillslopes and channels) but, at least for the forecasting of floods, just a simple model works [see also, Shorussian et al] leading to the conclusion that the river systems should work to simplify statistically the complexity underneath. The big problem in the GIUH approach however was (and is) the determination of the effective rainfall, i.e. the correct separation of surface runoff (interpreted as the cause of the flood surge) from subsurface flow (which must be actually treated separately and routed to the channels in a slower way), especially in dependence of storm events of diverse intensity, duration and inter-arrival time. A model more or less contemporary to the GUH is the TOPMODEL by Beven and Kirkby [1979]. It is based on the paradigm that runoff production is due to saturated areas (according to Dunne and Black, 1970). Thus once one knows which areas are saturated and describes their growing during an event, the problem of the runoff coefficient is 90 percent solved while routing of water to an outlet can be accomplished by some simple mechanism (the Muskingum-Cunge model at least in the original papers). An idea could have been to merge the best of the two formulations, the GIUH concept with the TOPMODEL. However the hypothesis on which the TOPMODEL has been based, mainly the stationarity of the hillslope subsurface fluxes, on the one hand simplifies the life of the modeler, but on the other is from many points of view a limitation which needs several work-arounds [Beven et al, 2002]. When the final goal is not simply the production of a well-fitted flood wave, but for instance the estimation of local soil moisture contents, the TOPMODEL fails to be precise enough [Grayson and Wilson, 2002]. Furthermore, the parameters entering the model become "effective" parameters and lose their original physical significance (e.g. the hydraulic conductivity cannot be validated by field measurements). Other limitations will be mentioned below when talking about the GEOTP$_{0.875}$ version. In any case, the TOPMODEL concept has been demonstrated to be a good tool to model floods in small-to -medium catchments, and has been considered the reference hydrological model for many of the researchers during the '90s. The TOPMODEL's ability to forecast floods derives also from its account (trivial indeed) of the topology and geometry of small- catchment flow paths: it was shown, in fact, that in small watersheds (up to at least 1000 square kilometers), hillslope residence time dominates the characteristic time of flood formation and that topology and geometry of river basins are sufficient with very minimalist dynamics to explain the shape of floods [Rinaldo et al, 1991; Rigon et al, 1996, Rinaldo et al., 1995, D'Odorico, 1996; D'Odorico and Rigon, 2003].

Thus, we decided to build a completely new subsurface and surface model, still

driven by gravity (i.e. by slope as the TOPMODEL and not by the total hydraulic head) but, as a first approximation to the final wishes, introducing the buffer due to infiltration into the vadose zone, while subsurface flow was produced only by the saturated layer, if present, and lateral surface runoff was routed as a kinematic wave (and through Manning/Gauckler-Strikler equation for velocities). In doing this, we searched for a better characterization of flow paths, with reference to the bedrock, instead of to the surface topography [see McDonnell et al., 1996] : this could be done by measuring soil depth or interpolating it for instance as in [Heimsath et al, 1997 or Roering et al, 1999; see Bertoldi et al, 2002 for the details]. In this separation GEOTOP is similar to the grid bases THALES [Grayson et al., 1994a,1994b] or NEWTHALES []. At first, the version of GEOTOP by Verardo-Pregoretti-Rigon (GEOTOP$_{0.5}$) could work without an explicit channel routing assigning a locally variable roughness and hydraulic radius; however channels were determined by accurate topographic analysis and explicitly treated. Channels routing is performed by a GUH theory as in Rinaldo et al [1991], where channel celerity and hydrodynamic dispersion are considered temporally and spatially constant. Instead of the effective rainfall, the spatially an temporally distributed input to channels produced by GEOTOP was considered.

The GEOMODEL produces patterns of spatially distributed soil moisture and these patterns are used to reduce the potential evapotranspiration to its real counterpart as described in Bertoldi et al, [2002].

1.1.1 GEOTOP$_{0.75}$

(mostly financed by COFIN 2001, THARMIT Eu Project, CUDAM - CofinLab 2001, ASI 54/2000)

The use of Penman-Monteith (PM) equation was unsatisfactory from many points of view. I would like to eliminate the parametrization of fluxes into the ground (which must be sensitive both to the ground cover and to the water content); moreover, the air surface temperature was still very uncoupled to the dynamic of hydrological fluxes at the surface and was more or less the gluing of PM equations to a distributed rainfall-runoff model. Using an image of Dietrich et al [2003], we can say that it is a picture where all the elements are realistic but the whole picture is a landscape of fantasy as the painting of Rosseau in Figure 1. As a result, many of the variables and parameters that are known to be correlated were actually treated separately. Thus, with the Master thesis of Giacomo Bertoldi[2000] we decided to throw away the PM equation (actually we kept it for comparison) and to solve directly the energy balance in any point of the basin. This was the birth of GEOTOP$_{0.75}$ which is thoroughly documented in Bertoldi et al[2002a,b] and Rigon et al [2002]. It is actually a SVATS model plus an rainfall-runoff model coupled together. GEOTOP$_{0.75}$ needs several parameters to be run, however the SVAT part has no more parameters than a normal SVATS model. The same applies to the rainfall-runoff parts. Thus, at least at first, the user can switch-off the SVATS part and have a parametrically parsimonious rainfall-runoff model, or vice-versa he can switch-off the rainfall-runoff model and have a reasonably simple SVATS model. Since some parameters concur to determine the dynamics of both the lateral and the vertical fluxes when both the components are on, GEOTOP must fulfill more strictly physical consistency requirements that usual models do. Large efforts were also done in cleaning the old code and improving the input-outputs. Credits must be given to the work of Lettenmaier et al [] with their work on VIC (which is however parametrized to work at much larger scales) and on Wigmosta et al. [] whose model is very similar to the version 0.75 of GEOTOP (but was mostly a case of evolutionary convergence since the comparison came after the GEOTOP actual implementation).

From the beginning, Giacomo and I did not want to limit the model only to the forecasting of floods; we wanted to have a tool which let us control the whole hydrological cycle continuously in time, and being comprehensive of snow cover, soil temperature and freezing and all of those properties which make it possible, in perspective, to cope with the ecosystem of plants out of balance because of the evolving climate or of the human-changed environment. Eco-hydrology was, in fact, a research thread whose seeds where already in Rodriguez-Iturbe's mind when I was working with him at the Texas A&M University [1994-1996] and of which I was concerned from the beginning of the GEOTOP project. Ecohydrology [Rodriguez-Iturbe, 2000, XXXX] has roots in the work of Eagleson [1978, 2003], Philip [e.g. XXXXX], Brutsaert [], Hillel [1990] and many others and is one of the hot issues in this hydrological decade [Rodriguez-Iturbe, 2000]. GEOTOP can work with a few parameters (made constant all over the basin) but to make use of all the features included in GEOTOP and to test the validity of the modules implemented we needed to refer to extensive field measurements. A key role in this had Tom Over who, besides giving a lot of suggestions making the concepts behind the model clear, suggested to use the South Great Planes 97 experiment data set, thing that we promptly did as it appears in the first papers published on GEOTOP.

Together with GEOTOP$_{0.75}$ also [Bertoldi et al, 2002a, 2003; Rigon et al, 2002] were produced and also the hydrological balance simulations in Bertola et al., [2002]. GEOTOP$_{0.75}$ was the base for the subsequent evolution (mostly financed by MIUR-COFIN2001) which brought to the actual branches of development which are converging into GEOTOP$_{0.875}$.

1.2 GEOTOP$_{0.875}$

(mostly financed by TIDE EU Project, CUDAM Cofinlab COFIN 2001, THARMIT EU project)

This new version finally contains a snow accumulation melt model (derived by the Utah Energy Balance -UEB- by Tarboton and Luce, [1992]) implemented by Fabrizio Zanotti [2003]. It also includes a post-processor program, the S-FACTOR, which performs a landslide and debris-flow triggering implemented by Christian Tiso [2003]. Both implementations were two Master Thesis under Giacomo's and my supervision. Snow-melting and soil freezing are essential components in the hydrological cycle of mountain catchments and could not be overlooked. Landslide and debris-flow triggering are also an issue with particular relevance on human activities. Floods in mountain areas are usually the combined effect of large liquid and solid discharges whose effects cannot be separated: GEOTOP can be a tool for getting some further insights in the next future.

With the version 0.875, we also would like to face some other relevant hydrological questions: mainly those well described in Kirchner [2003]. Our understanding of mountain catchments in fact is based on hillslope zone hydrology (as reviewed for instance in Wipkey and Kirkby [1978]). The 'perceptual' hillslope model that derives from these concepts is based on the following assumptions: that it is possible to neglect the transients in the water fluxes [in the sense clarified in Iverson, 2000], that topographic gradients dominate the hydrologic response, that hydraulic conductivity strongly decreases with depth in the soil and, not independently, that runoff occurs mostly owing to saturation excess. This last assumption is based on the results of a long series of experiments from the late seventies on by American geomormologists (Dunne, Black, Dietrich, Montgomery, Torres), and it is also supported by many others (among these: Moore, Grayson, Sivapalan, Wood). These experiments changed the be-

lief spread by Horton that runoff was mostly due to an infiltration excess mechanism. Developing hydrological models based on saturation excess ideas (which involved further simplification) originated a series of rainfall-runoff models among which the already cited TOPMODEL [Beven and Kirkby,1979; Sivapalan et al, 1991; Franchini et al, 1996] is the most successful product. Sharpening our inspection, however, we have to say that TOPMODEL and experimental hillslope hydrology do not constitute a really monolithic and internally consistent theory (when modeling is concerned, parameters -usually the hydraulic conductivity- are fitted to values very different from those measured locally on the field [Dietrich et al, 1995] and many empirical observations do not match [Kirchner, 2003] with model findings). There are many aspects we would improve in the modelling of the hydrological cycle but with GEOTOP$_{0.875}$ we focused mainly on 2 of them:

[1] - The conceptual separation of hillslope and buffer zones. The latter are alluvial fans and low-gradient areas where more or less stable aquifers form (e.g. Herron et al, 2000; Buttherworth et al, 2000; Seibert et al, 2003). These zones play an important role in interstorm soil moisture redistribution and hence in runoff generation, but also in the dynamics of floods. We expect that these "buffer" zones can be extracted from Digital Elevation Models by objective techniques and separated from hillslopes (it is worth mentioning that most of DEM data currently available were produced by "digitization", i.e. from data originally stored in conventional maps, and not, as required by objective techniques, generated directly in digital form as it would be true for laser altimeter or SRTM data).

[2] - The characterization of the subsurface flow field more in terms of total head ($\nabla z + \psi$), even if in simplified form as in Iverson [2000], than in terms of the topographic gradient. The rationale for this choice is partially contained in point 1 (above) and in the need for a correct account of the transient effects in subsurface flow during the storm period, usually neglected but clearly important to determine the subsurface flow and conditions (the total head gradient can increase locally by up to an order of magnitude, as revealed by our preliminary analyzes). These last steps were implemented by the master thesis of Davide Tamanini [2003].

1.2.1 What is next (GEOTOP$_{0.9375}$ and beyond)

(mostly financed by TIDE EU Project, ASI 2002, UT Fondi per la ricerca fondamentale and hopefully by COFIN 2003, FISR-CLIMIMPACT, Catch-Risk EU project, EU AQUATERRA Integrated project)

GEOTOP uses standard meteorological measurements, which are easily available at regular time intervals. However, GEOTOP has been implemented to be able to assimilate satellite and remotely-sensed hydro-meteorological data and to be coupled to local circulation atmospheric models. The next evolution of GEOTOP will include:

[1] - a better description of the vegetation, especially as to the transpiration mechanisms of different plant species during their vegetative life and the changing hydrological conditions (which, in turn, can affect the vegetation evolution);

[2] - a better regionalization of the hydrometeorological parameters which should include a simplified ABL modelling and some upscaling (and downscaling) interface to the micrometeorological models (as WRF, LOKALMODEL or other);

[3] - A first investigation on the assimilation of multitemporal satellite data regarding soil moisture content, vegetation and soil cover with the goal of integrating the traditional hydrological local measurements, both in input (e.g. pluviometers or local measurements of humidity) as well in output (e.g. discharges).

[4]- A systematic application of GEOTOP$_{0.875}$ to the case studies of Fiumarella (PZ), Tovel(TN), Zero (VE), Aquabona(BL) and Centa (TN) basins and some other small basins located in Trento Province.

[5]- Last but not least, a better theoretical frame for all the processes will be developed: a) to face consistently the problem of the heterogeneity of parameters following the stochastic frameworks developed in the groundwater field (e.g. Dagan, 1989, D. Zhang, 2001, Sposito, 1997) and b) to include the second law of thermodynamics into hydrology, based on the work by Reggiani et al. [1999].

Task 1 will be performed under the financial support (hopefully) of the FISR-CLIMIMPACT. Task 2 with the financial support of TIDE and (hopefully) of the COFIN2003. Task 3 with the financial support of ASI/2001 and hopefully of an integrated European Project. Task 4 is financed by COFIN 2001 (Fiumarella 2001), Cofinlab 2001 (Tovel, Aquabona and Centa), TIDE (Zero), ASI (Aquabona and Centa), Caldonazzo (PATT); other (PATT-CatchRisk). Simulations on Aquabona, Centa and other will be mostly devoted to the determination of sediment fluxes and landslide-debris flow triggering.

Task 1 will be pursued first with the use of a local model developed mostly by Emanuele Cordano in his Ph.D work at the University of Genoa, and validated in the infrastructure of the CLIMIPACT FISR project. Though slowly, the acquired knowledge will flow into GEOTOP and it will be used mostly following the footsteps of Rodriguez-Iturbe, Porporato and Ridolfi's type of analysis.

As regards task 2, there is a scale gap among the micro-meteorological models and the GEOTOP. Micrometeorological models of the last generation works with the physics parametrized at some-hundreds-meter-to-one-kilometer grid size, while GEOTOP works at ten-to-one-hundred meters grid size and the subgrid parametrization lumps phenomena work at a scale of few square meters. Moreover: a - the regionalization of some relevant parameters (especially winds, air temperature close to the terrain and atmospheric optical thickness) are still in the highly simplified form provided by GEOTOP$_{0.5}$ inheritance; b - We would like to account much better for turbulence development and exchanges.

We believe that this operation is necessary not only to complete the description of the hydrological cycle processes but also to improve the actual LAMs predictions, since it is clear that their performances are strongly affected by the local water budget (Liang X., Lettenmaier P., Wood E. F., Burges S. J., 1994) which, in turn, is very dependent on microtopography and evapotranspiration (Bertoldi et al, 2002).

Remote-sensed data are the natural data sets for distributed hydrological models since they let us compare directly the spatial distribution of soil moisture of large areas to that provided by the model, and make it possible to use distributed rainfall input data (just to cite to quantities related to runoff formation) or the distribution of soil temperature (which has effects on the hydrological cycle but also on vegetation). It is clear that remote-sensed data are obtained through a model itself, since the quantity directly derived is another (for instance the soil moisture is deduced as brilliance temperature) and this makes the remote sensing and the hydrological models a concurrent experiment in which the hydrological model is also useful to calibrate the measurements. Obviously both of them require ground truth and at least some local calibration points. The distributed modeling as that in GEOTOP is in a sense an answer to the modelling demand coming from the next remote sensing mission, among which the ENVISAT and the Italian COSMO-SkyMed. Such satellites will make it possible to shorten greatly the visiting time of the satellites on a single area (from weeks to days or hours), and to have a broader spectral quality and resolution of the sensors. Parallel to

the hydrological modelling is the present emphasis on improving the new methodologies for the automatic acquisition and interpretation of sensor data especially to refresh the thematic maps available and to reveal the surface changes in real time (above all those which can be related to an environmental disaster or hazard).

As far as I can foresee, the application of GEOTOP on large basins, using parallel computers and connecting the single "basin units" by an explicitly modelled channel network where fluxes are solved by integration of 1D or 2D de Saint Venant equation. However, much basic work still remains to do in understanding the fundamental laws of transport in hillslope, and plans, and in coupling quality models and with large scale hydrological model. At the point GEOTOP will be probably really able to run forever and give real time information of the hydrological fluxes and quantities everywhere.

However, the topics described before will not shade the necessity to deepen our knowledge about the fundamental hydrological processes in the whole hydrological cycle. New insights as well new technologies will obviously move the focus of the research and GEOTOP evolution.

With respect to this, a fundamental role will be played also by the decision to let GEOTOP be an Open source code to which all interested researchers will be able to contribute.

Riccardo Rigon

Chapter 2

Introduction

GEO_{TOP} is a distributed model of the mass and energy balance of the hydrological cycle, which is applicable to simulations in continuum in small catchments. GEO_{TOP} deals with the effects of topography on the interaction between energy balance and hydrological cycle with peculiar solutions. In this manual is explained the the theoretical backgound, the model's structure, the code organization, the input and output files and some applications examples.

2.1 Background

The purpose of the distributed hydrological model $\mathrm{GEO_{TOP}}$ is to estimate in an integrated way the rainfall-runoff and the energy fluxes, with particular attention to evapotranspiration in small mountain catchments.

Such a model satisfies the requirements of a modern management of the water resources and of the hydrogeological risk and could use the modern tools offered by DEMs (Digital Elevations Models) and data as those produced in specialized measurement campaigns like FIFE (First ISLSCP Field Experiment, *Sellers et al., 1992*), PILPS (*Heanderson-Sellers and Brown*, 1992), HAPEX-MOBILHY (Modelisation de Bilan Hydrique, *Andrè et al, 1988*), SGP97, Tarrawarra (*Western et al., 1998*), DMIP (Distributed Models Intercomparison Project,
http://www.nws.noaa.gov/oh/hrl/dmip/), MARVEX (*Woods, 1997*), to mention a few experiments only.

In the last thirty years several distributed hydrological models have been developed and, independently, models of soil-atmosphere interaction for the computation of the energy balance at the soil. Actually, the inflow-runoff models based on the paradigms of the unitary instantaneous geomorphological hygrograph (IUH) (*Rodriguez-Iturbe e Valdes*, 1979; *Rodriguez-Iturbe e Rinaldo*, 1997), of the TOPMODEL (*Beven e Kirkby*, 1979), and other distributed and semi-distributed models like the THALES (*Grayson et al.*, 1995) or the TOPKAPI (*Ciarapica e Todini*, 1998) and many more reported in *Beven* (2000), are successful in the flood events modelling (assuming opportune conditions of initial moisture and/or calibrating some other parameters, generally two or three), but they are generally unable to follow the runoffs evolution in the time after the floods and, obviously, to estimate evapotranspiration precisely enough.

Viceversa, also numerous models LSMs (Land Surface Models) have been developed: they represent the soil-atmosphere interactions with a different degree of com-

plexity and accuracy, from the simple bucket model (*Manabe*, 1969), to a complex representation of the multilayer vertical interactions like the models BATS (*Dickinson et al.*, 1986), SiB (*Sellers et al.*, 1986), VIC (*Wood ed al.*, 1992), NOAH-LSM (*Mitchell et al*, 2000). Nevertheless, having been developed mainly to support the global circulation atmospheric models (GCM), they are not endowed with a detailed representation of the superficial hydrological processes at catchment scale.

$\mathrm{GEO_{TOP}}$ can be seen both as an inflow-runoff model able to simulate the hydrological cycle with continuity during the time, and as an attempt to incorporate in the LSMs an adequate treatment of the hydrological variability on a small scale, in particular the effects due to an use of the heterogeneous soil, to the spatial distribution of the soil moisture, and to the presence of a complex topography and of a channel network.

2.2 Model Description

The model $\mathrm{GEO_{TOP}}$ simulates the complete hydrological balance in a continuous way, during a whole year, inside a basin and combines the main features of the modern land surfaces models with the distributed rainfall-runoff models.

$\mathrm{GEO_{TOP}}$ makes it possible to know the outgoing discharge at the basin's closing section, to estimate the local values at the ground of humidity, of soil temperature, of sensible and latent heat fluxes, of heat flux in the soil and of net radiation, together with other hydrometeorlogical distributed variables.

$\mathrm{GEO_{TOP}}$ is a model based on the use of Digital Elevation Models (DEMs). It makes also use of meteorological measurements obtained thought traditional instruments on the ground. Yet, it can also assimilate distributed data like those coming from radar measurements, from satellite terrain sensing or from micrometeorological models.

As any distributed grid based model, it divide the watershed in cells (sometimes called pixels). For every cell, the model solves both the energy and the water balance, divided in lateral and vertical flows.

The lateral runoffs are moreover distinguished in a surface component with a faster motion, and a subsurface component with a slower motion, linked to the local slope.

The soil water content is divided in an unsaturated upper zone, characterized by the development of a vertical infiltration process, and an saturated lower zone, in which there is a motion parallel to the rocky slope considered to be an impermeable surface. If the rain intensity is higher than the saturation hydraulic conductivity, or if the water table level reaches the surface, there can be surface runoff, according to the mechanism illustrated in Fig. 2.1.

An important variable of the model is the thickness of the hillslopes' hydrologically active soil which is determined, if field values are not available, on the basis of a linear model of soil production (Hiemsath et al, 1997, Stocker, 1998).

All the basin's cells are divided in channel and hillsides cells. The surface runoff in the hillsides is described as a succession of uniform motions and the subsurface flow is on the basis of Darcy's law. In both cases, the connectivity among the cells is defined by the D8 scheme, with eight drainage directions (Fairfield and Leymarie, 1991).

The channel network is build from the DEM using a stress method (Prosser and Abernethy, 1996). The motion inside the channels is described by the parabolic solution of the De Saint Venant equations, by using a constant celerity in the whole network as proposed in (Rinaldo et al., 1991) and globally described by the:

$$Q(t) = \int_0^t \int_0^L \frac{xW(\tau, x)}{\sqrt{4\pi D(t-\tau)^3}} \exp\left[-\frac{(x-u(t-\tau))^2}{4D(t-\tau)}\right] d\tau \cdot dx \quad {}_{(1)} \qquad (2.1)$$

where $Q(t)$ is the discharge at the basin's closing section , $W(t, x)$ is the inflow of the water coming from the hillsides into the channel network at a distance x from the outlet and at a time t, u an opportune mean celerity, D a hydrodynamic dispersion coefficient, L the maximum distance from the outlet measured along the network.

The model calculates in an explicit way the energy balance as a function of the soil temperature, and by numerically solving the equation:

$$\frac{\Delta E}{\Delta t} = R_n - H - ET - G \quad {}_{(2)} \qquad (2.2)$$

where R_n is the net radiation, H is the sensible heat flux, ET the evapotranspiration, G the heat flux towards the soil, and E the internal energy of the surface layer.

The radiation is distinguished in its long- and short-wave components, diffused, directed and reflected, both emitted by the land and shielded by the cloud cover.

The effects due to the mountain relief are taken into account: the shadowing, the net radiation variation as a function of exposition and slope, and the reduction of the sky view factor.

The air temperature, the atmospheric pressure and the solar radiation absorption are connected to the elevation according to relations valid in a standard atmosphere (Brutsaert, 1982).

The heat flux in the soil is calculated through the integration at the finite differences of the conduction equation, with an implicit scheme on an arbitrary number of layers (Garrat,1992).

The soils capacity and thermal conductivity are made dependent on the soil water content, which is variable during the time like in the soil water content, which is variable during the time like in

The sensible and latent heat fluxes are determined through flux-gradient relations between two reference quotes.

$$H = \rho c_p C_H u(T_s - T_a) \qquad (2.3)$$

$$EP = \rho C_H u(q^*(T_s) - q(T_a)) \qquad (2.4)$$

The sensible heat flux $H$is expressed as a function of the atmospheric turbulence through the bulk coefficient C_H, of the wind velocity u, of the gradient between soil temperature T_s and air temperature T_a, while potential evapotranspiration is expressed as a function of the gradient between saturation specific moisture at the soil $q^*(T_s)$ and specific air moisture $q(T_a)$.

The bulk coefficient C_H, which encloses the turbulent transfer processes, takes into account the different roughness features of the various surfaces, through a mapping of the soil use and of the stability or instability atmospheric conditions, which inhibit or force the turbulent motions. C_H is expressed according to Louis' theory (1979), which uses as stability parameter the Richardson number, expressed as a function of the potential temperature gradient between soil and atmosphere.

The local ratio between real evaporation *ET* and potential evaporation is controlled by the soil water content, as suggested by Eagleson (1970):

$$ET = xEP \tag{2.5}$$

where x is linked to the soil saturation *sat* according to the:

$$x = min(1; sat/0.75) \tag{2.6}$$

The soil saturation is referred to the soil thickness as a whole, therefore it is given by the ratio between all the flooded volume (upper unsaturated volume and lower saturated volume) and the total volume of the vacuums as showed in Fig. 2.1.

The latent heat fluxes are distinguished in evaporation from the land, transpiration on behalf of the vegetation, evaporation of the precipitation intercepted by the vegetation.

To every cell is attributed a fraction covered by vegetation and a fraction covered by bare soil, where the evaporation is calculated with the (2.6).

A one-level model of vegetation is employed, as in Garrat (1992) and in Mengelkamp et al.(1999). Only one temperature is assumed to be representative of both soil and vegetation.

The energy balance of the hydrological bodies is calculated with a specific scheme, in order to take into account the different absorption of the solar radiation and the turbulent heat transport inside them.

The model has been successfully applied and tested in some mountain watershed of Trento Province in Italy and is some well monitored basins in the USA of different sizes ($10 - 1000\ km^2$).

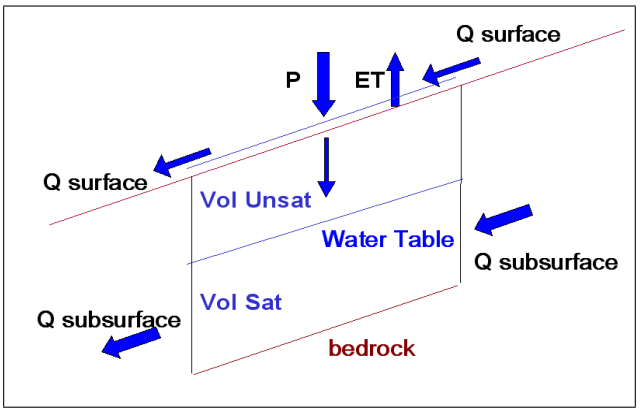

Figure 2.1: *The fluxes partition scheme used in the GEO$_{\mathrm{TOP}}$ model. In every cell, the precipitation (P) is divided in evaporation (ET), subsurface runoff (Qsub) and surface runoff (Q sup). The latter can be due both to a rain intensity greater than the infiltration velocity, with the formation of a thin layer of water on the surface, and to the water table ascent. In the model the infiltrated volumes move downward with a constant velocity (Vol Unsat), until they reach the bedrock, which is assumed to be impermeable. The dynamic balance between lateral flows (Qsub) and vertical flows (Vol Unsat) determines the water table level. Both the upper unsaturated (Vol Unsat) and the lower saturated volume (Vol Sat) contribute to the evaporation, while only the saturated volume contributes to the lateral flows.*

Chapter 3

Technical Description

In this chapter we will briefly describe how the model calculates the parts of the hydrological balance.

3.1 Precipitation

Precipitations can be detected through radar data, or it can be interpolated from raingage measurement. The programs use the kriging method (Kitanidis, 1997) for the spatial interpolation. Moreover the effect of the canopy interception for different land cover classes is taken into account.

3.1.1 Spatial Interpolation of Precipitation

If more raingages are available, the spatial interpolation of precipitation is obtained by using the kriging method (Kitanidis, 1997).

If the precipitation on a regular grid is known, the program interpolates the measurement ($\mathrm{Z(x_1)}$, $\mathrm{Z(x_2)}$ ... $\mathrm{Z(x_n)}$) made in n points.

The measurements are supposed to be a stationary and isotropic stochastic field, using an exponential variogram, such as:

$$\gamma(r) = \sigma^2 \left(1 - \exp\left(-\frac{r}{L}\right)\right) \tag{3.1}$$

where r is the distance between the measurement points, L is the integral scale, σ^2 the variance. These values are given as input.

For each grid point x_0, the program solves the system:

$$\overline{\overline{A}} \cdot \overline{\lambda} = \overline{b} \tag{3.2}$$

$$\overline{\overline{A}} = \begin{bmatrix} 0 & \gamma(x_1,x_2) & ... & \gamma(x_1,x_n) & 1 \\ \gamma(x_2,x_1) & 0 & ... & \gamma(x_2,x_n) & 1 \\ ... & ... & ... & ... & ... \\ \gamma(x_n,x_1) & \gamma(x_n,x_2) & ... & 0 & 1 \\ 1 & 1 & ... & 1 & 0 \end{bmatrix} \quad \overline{\lambda} = \begin{bmatrix} \lambda_1 \\ \lambda_2 \\ ... \\ \lambda_n \\ \mu \end{bmatrix} \quad \overline{b} = \begin{bmatrix} \gamma(x_0,x_1) \\ \gamma(x_0,x_2) \\ ... \\ \gamma(x_0,x_n) \\ 1 \end{bmatrix} \tag{3.3}$$

where $\overline{\overline{A}}$ is the matrix with the variogram between the measurement points, $\overline{b}$ is the vector with the variogram between the grid point x_0 and the measurement points, and $\overline{\lambda}$ is the weight vector.

The system is numerically solved, using the method of the decomposition L-U.

When the weight vector is known, the estimated value in the grid point will be:

$$Z(x_0) = \sum_{i=1}^{n} \lambda_i Z(x_i) \tag{3.4}$$

3.1.2 Canopy Interception

The canopy interception of precipitation is solved according to Deardorff (1978), developed later by Mengelkamp et al. (1999).

The depth of the intercepted water w_r is given by:

$$\frac{\partial w_r}{\partial t} = veg\ P - E_{vc}\ veg\ \delta_w \tag{3.5}$$

where P is the precipitation, veg is the surface fraction covered by vegetation , E_{vc} is the evaporation from the leaves and δ_w is the wet canopy fraction given as a power function of w_r:

$$\delta_w = \left(\frac{w_r}{w_{r\ max}} \right)^{2/3} \tag{3.6}$$

the maximum water storage is given by:

$$w_{r\ max} = 0.2\ veg\ LAI \tag{3.7}$$

The (3.5) is valid only if $0 \leq w_r \leq w_{r\ max}$: if $w_r > w_{r\ max}$ the precipitation P_{eff} reaches the soil:

$$P_{eff} = \frac{w_r - w_{r\ max}}{\Delta t} \tag{3.8}$$

3.2 Air Temperature and Pressure

The atmospheric pressure and the air temperature, measured in one or more meteorological stations, are related to elevation. If more temperature measurements at different elevations are available, a linear interpolation is used. If they are not, a standard atmosphere model, valid in neutral stability conditions, is used.

- Pressure (Brutsaert,1982):

  $$P(z) = P_{staz} exp(-(z - z_{staz}) * 0.00013) \tag{3.9}$$

  with: z local elevation [m], z_{staz} station elevation, P_{staz} measured pressure [hPa].

- Air temperature [^oC]:

  $$T_a = (T_a + 273.15)\ exp(-(\Gamma_T/(T_a + 273.15))(z - z_{staz})) - 273.15 \tag{3.10}$$

  a quasi-linear exponential relationship with $\Gamma_T = 0.006509$ [K/m].

is assumed.

3.3 Solar Radiation and Shadows

The matter is extensively explained in Iqbal (1983). Here only the principal equations used by the model are reported.

The position of the Sun is calculated firstly by using the relations:

- daily angle:

$$\Gamma = \frac{2\,\pi\,(d_n - 1)}{365} \tag{3.11}$$

- correction of the Earth-Sun distance:

$$E_0 = 1.00011 + 0.034221\cos(\Gamma) + 0.00128\sin(\Gamma) + 0.000719\cos(2\Gamma) + 0.000077\sin(2\Gamma) \tag{3.12}$$

- solar declination:

$$\begin{aligned}\delta = {} & .006918 - .399912\cos(\Gamma) + .070257\sin(\Gamma) - .006758\cos(2\,\Gamma) \\ & + .000907\sin(2\,\Gamma) - .002697\cos(3\,\Gamma) + .00148\sin(3\,\Gamma)\end{aligned} \tag{3.13}$$

- solar height (radians):

$$\alpha = arcsin(sin(\phi)sin(\delta) + cos(\phi)cos(\delta)cos(\omega \cdot t)) \tag{3.14}$$

- Suns azimuth (from North, hourly direction, radians):

$$\psi = \begin{cases} \pi & \text{se } t = 0 \\ \pi + \frac{t \cdot \arccos(\frac{\sin(\alpha)\sin(\phi) - \sin(\delta)}{\cos(\alpha)\cos(\phi)})}{|t|} & \text{se } t \neq 0 \end{cases} \tag{3.15}$$

Definitions and angle sign convention are the following:

α	solar height (angle between the Sun and the horizon) [rad];
$\omega = 0.2618$	Earth angular velocity [rad/h];
$t = ora - 12$	local hour relative to the solar noon;
ϕ	latitude [rad];
ψ	Sun's azimuth, zero Nord, hourly direction [rad];
δ	solar declination [rad];

The program then calculates the shadows of the reliefs given by the DEM, by using a very efficient algorithms (Verardo, 1998). The basic idea is that only convex cells can create shadow on the other cells.

The incoming shortwave radiation can be calculated in different ways, depending on the data availability:

1. No radiation measurement.
2. Only global shortwave radiation measurement $R\downarrow_{SW\ glob}$.
3. Diffuse shortwave radiation measurement, $R\downarrow_{SW\ diff}$.
4. Longwave radiation measurement, $R\downarrow_{LW}$.

If the radiation measurements are not available, empirical expressions are used to calculate the attenuation of the extraterrestrial radiation due to atmosphere and to cloud cover:

- extraterrestrial radiation:

$$R_{ext} = I_{sc} E_o sin(\alpha)\ att_n\ att \tag{3.16}$$

con $I_{sc} = 1367W\ m^{-2}$.

- attenuation due to the cloud cover (Reiff et al., 1984):

$$att_n = \frac{R_{SW\downarrow}}{R_{SW\ clear}} = (1 - c_1 N_2^c) \tag{3.17}$$

dove $c_1 = 0.6$, $c_2 = 2.5$ (calibrated on experimental data).

- atmospheric attenuation:

$$att = \frac{R_{SW\ clear}}{R_{SW\ extr}} = \cdot sw \cdot \exp(-n\ a_1\ m_r) \tag{3.18}$$

with sw (0 if the pixel is in the shade, 1 if it is in the sun), $n = 2$ torpidity factor and $a_1 = 0.1$ molecular dispersion factor (Eagleson, 1970).

- optic mass (Paltrige e Platt, 1976)):

$$m_r = \frac{1}{\sin(\alpha)} \frac{P}{P_0} \tag{3.19}$$

with α solar heght, P atmospheric pressure, $P_0 = 1013\ hPa$.

If radiation measurements are available, then the 3.18 is used only to take into account the different absorbance at different elevations, using a linear relationship with the optical mass.

- atmospheric attenuation calculated with the pressure at the pixel elevation (Eagleson, 1970):

$$att = \exp(-n\ a_1\ m_r) \tag{3.20}$$

- global shortwave radiation at pixel height:

$$R\downarrow_{SW} = R\downarrow_{SW(quota\ stazione)}\ \ att/att_{staz} \tag{3.21}$$

If the diffuse radiation is measured separately, in the generic pixel it can be expressed as:

$$R\downarrow_{SW\ diff} = R\downarrow_{SW\ diff(quota\ stazione)}\ \ att/att_{staz}\ V/V_{staz} \tag{3.22}$$

where V and V_{staz} are the sky view factor in a generic pixel and in the measurement station respectively.

If the diffuse radiation is not measured, the following expression, calibrated on experimental data, is used:

$$\begin{aligned} R\downarrow_{SW\ diff} &= (0.1 + 0.8\ N_{tot}) \cdot \\ &\cdot \quad R\downarrow_{SW\ globale} /sin(\alpha)\ att/att_{staz}\ V \end{aligned} \tag{3.23}$$

with N_{tot} sky fraction covered by clouds. The diffuse radiation has to be less than the global radiation, and if the angle of the Sun on the horizon is less than 5^o, then the whole radiation is considered to be diffuse.

The radiation is related with the local slope and aspect (Iqbal, 1983):

$$R\downarrow_{SW} = sw\ (R\downarrow_{SW(pianoorizzontale)} - R\downarrow_{SW\ diff})\cos(\theta)/sin(\alpha) + R\downarrow_{SW\ diff} \tag{3.24}$$

with $sw = 0$ if the pixel is in the shade, $sw = 1$ elsewhere, $\cos(\theta)$ cosine of the solar incidence angle.

$$\cos(\theta) = \cos(\nabla z)\cos(\frac{\pi}{2} - \alpha) + \sin(\nabla z)\sin(\frac{\pi}{2} - \alpha)\cos(\gamma - \psi) \tag{3.25}$$

where ∇z is the local slope [rad] and γ is the local aspect (zero North, hourly direction [rad]).

3.4 The Energy Balance

The calculation of the energy balance is based on the measurement of u, T_a, U_r, P, $R\downarrow_{SW}$; all these data are usually quite easy to obtain. To be clearer, in the following paragraph the measured quantities will be indicated with: $\hat{}$.

The model solves the energy balance keeping the soil temperature as unknown variable. The balance equation can be expressed as function of the soil heat flux G $[W/m^2]$, and than, integrating the differential equation of conduction, the correct soli temperature is found.

$$G(T_s) = R_n - H - \lambda ET - \frac{\Delta E}{\Delta t} \tag{3.26}$$

In the next paragraphs the components of the (3.26) will be explained.

3.4.1 Net Radiation

The net radiation R_n $[W/m^2]$ is expressed, without the effects of the sky view factor, as:

$$R_n = \hat{R\downarrow}_{SW}(1 - a) + \varepsilon_s R\downarrow_{LW} - \varepsilon_s \sigma T_s^4 \tag{3.27}$$

The shortwave radiation $R\downarrow_{SW}$ $[W/m^2]$ is assumed to be measured, a is the albedo (for grass between 0.1 and 0.3), ε_s is the longwave soil emissivity (values between 0.95 and 0.98), $\sigma = 5.6704 \cdot 10^{-8}$ $[W/(m^2K^4)]$ is the Stefan-Boltzman constant, T_s $[K]$ is the soil skin temperature, $R\downarrow_{LW}$ is the shortwave radiation, calculated according to Brutsaert (1975), valid in clear sky conditions:

$$R\downarrow_{LW} = \epsilon_a \sigma \hat{T_a}^4 \tag{3.28}$$

where $\hat{T_a}$ $[K]$ is the measured air temperature and ϵ_a is the emissivity for a standard atmosphere:

$$\epsilon_a = 1.24 \left(\frac{e_a}{\hat{T_a}}\right)^{1/7} \tag{3.29}$$

where e_a $[hPa]$ is the partial air vapor pressure, which is a function of the saturation pressure e_s (Bolton, 1980):

$$e_a = \hat{U_r} \cdot e_s \tag{3.30}$$

$$e_s = 6.112 \cdot \exp\left(17.67\ \frac{(\hat{T_a} - 273.15)}{(\hat{T_a} - 29.65)}\right) \tag{3.31}$$

Other empirical terms take into account the presence of cloud cover. The atmospheric emissivity ϵ_a increases of about 25% with sky completely covered by low clouds. With cloud cover, ϵ_a is corrected by the equation (Arnfield, 1979):

$$\epsilon_{a\ cloudy}/\epsilon_{a\ clear} = 1 + N_{TOT}(0.2N_H + 0.06(N_{TOT} - N_H)) \tag{3.32}$$

where N_{TOT} is the total cloud cover fraction, N_H is the low and mean cloud cover.

3.4.2 Internal Energy Variation

The energy fluxes are calculated at the same height as the wind measuremets. The energy E stored between the surface and the measurement height is not negligible if there is vegetation. The vegetation thermic capacity is estimated to be equivalent to a water amount of 2.5 cm/m^2, for a pine forest with a wood mass of about 600 m^3/ha.

The internal energy variation in the time step $\Delta E/\Delta t$ is given by the sum of soil-, vegetation- and air-contributions in the control volume considered.

$$\Delta E = C_s(T_s^{i+1} - T_s^i) + C_v(\hat{T_a}^{i+1} - \hat{T_a}^i) + C_a(\hat{T_a}^{i+1} - \hat{T_a}^i) \tag{3.33}$$

where C_s, C_v, C_a are respectively the soil, vegetation and air thermic capacity.

3.4.3 Sensible Heat Flux

The sensible heat flux H $[W/m^2]$ is calculated as a function of the temperature gradient, of the mean wind velocity U and of the heat transport coefficient C_H:

$$H = \rho\, c_p\, C_H\, \hat{u}\, (T_s - \hat{T_a}) \tag{3.34}$$

where T_s is the soil surface temperature, T_a is the air temperature at the reference height, ρ $[kg/(m^3)]$ and c_p $[J/(kg\ K)]$ are respectively air density and air specific heat.

$$\rho = \frac{\hat{P}[Pa]}{287.04\,\hat{T_a}} \cdot \Big(1 - e_a/\hat{P} \cdot (1 - 0.622)\Big) \tag{3.35}$$

$$c_p = 1005 + (\hat{T_a} - 250)^2/3364 \tag{3.36}$$

where $\hat{P}$ $[Pa]$ is the atmospheric pressure.

The heat transport is schematized in analogy with the momentum transport.

$$C_H = \frac{k^2}{\ln(z/z_0)\ln(z1/z_T)} \cdot FH \tag{3.37}$$

with $k = 0.41$ Von Karman's constant, z wind measurement height, $z1$ temperature measurement height, z_0 momentum roughness, $z_T \simeq \frac{1}{5} - \frac{1}{10}\, z_0$ heat roughness.

The factor FH takes into account the atmospheric stability through the bulk Richardson's number Ri_b according to Louis' theory (1979), developed by Kot and Song (1998): $FH > 1$ if $Ri_b < 0$ (stable atmosphere), $FH < 1$ if $Ri_b > 0$ (unstable atmosphere).

$$FH = f(Ri_b) \tag{3.38}$$

$$Ri_b = -\frac{g\, z(T_s - \hat{T_a})}{(T_s + \hat{T_a})/2\, u^2} \cdot f^2 \tag{3.39}$$

$$f^2 = \frac{(1 - z_0/z)^2}{z_1/z - z_T/z} \tag{3.40}$$

3.4.4 Evapotranspiration

The evaporation ET is calculated as a function of the potential evapotranspiration EP.

The potential evapotranspiration is calculated as:

$$EP = \rho\, C_E\, \hat{u}\, \left(q^*(T_s) - q^*(\hat{T_a})\hat{U_a}\right) \tag{3.41}$$

where $q^*(T_s)$ is the air saturation specific humidity at the surface and $q^*(T_s)$ is the air saturation specific humidity at the reference height. The specific humidity is the rate between the water vapor mass m_v and the humid air mass $m_v + m_d$:

$$q = \frac{m_v}{m_v + m_d} \tag{3.42}$$

The bulk coefficient C_E is equal to the heat coefficient C_H. This assumption is true only in stable conditions, as it is still quite difficult to get information regarding the relationship between C_E and C_H in unstable conditions. The latent heat of evapotranspiration λ [J/Kg] is expressed as a linear function of temperature, validated on experimental data (Brutsaert, pg. 41, 1982).

$$\lambda = 2501000 + (2406000 - 2501000)\frac{\hat{T_a} - 273.15}{40} \tag{3.43}$$

If the pixel is inside a lake, there is potential evaporation and the heat flux into the water is calculated with a different scheme, by using the conduction law with an equivalent turbulent diffusivity. Such diffusivity has been estimated, for Lake Serraia, to be of approximately 0.07 - 0.09 m^2/d (Nascimbeni, 1999). The integration has been made on a thicker depth (ten meters), to simulate the damping depth of the thermic wave by the water. A constant temperature, equal to the mean annual temperature, has been chosen as a boundary condition.

If the pixel is different from free water the evaporation is divided in three components:

- E_G: evaporation from bare soil;
- E_{TC}: transpiration from canopy ;
- E_{VC}: evaporation from wet vegetation;

Bare Soil Evaporation

The bare soil evaporation is expressed as a function of the potential evaporation:

$$E_G = x\, E_P\, (1 - cop) \tag{3.44}$$

where cop is fraction of soil covered by the vegetation and the rate x is expressed as:

$$x = min(1, sat/0.75) \tag{3.45}$$

If it is free water on the surface, $x = 1$.

The soil is divided in a unsaturated upper layer and in a saturated lower layer (see fig. 7.7).

The soil saturation is calculated as:

$$s = \frac{Vol_{uns} + Vol_{sat}}{Vol} \tag{3.46}$$

where Vol_{uns} is the water volume in the unsatured upper layer, Vol_{sat} is the water volume in the lower satured layer and Vol is the available volume in the soil, given by:

$$Vol = \theta_s \cdot h_s \cdot A \tag{3.47}$$

where θ_s is the porosity, h_s is the soil thickness and A is the pixels area.

The spatial and temporal distribution of soil moisture is controlled, besides the atmospheric forcing, from the lateral subsurface flow in the saturated lower layer.

Wet Vegetation Evaporation

The evaporation from wet vegetation is calculated as:

$$E_{VC} = cop\ E_P\ \delta_W \tag{3.48}$$

where δ_W is the wet vegetation fraction (Deardorff, 1978):

$$\delta_W = min\left(1, \left(\frac{W_r}{W_{r\ max}}\right)^{(2/3)}\right) \tag{3.49}$$

with $W_{r\ max}$ maximum interception (about 4 mm).

Dry Vegetation Evaporation

The transpiration from dry vegetation is calculated as:

$$E_{TC} = cop\ E_P\ r_a/(r_a + r_c)(1 - \delta_W) \tag{3.50}$$

with $r_a = 1/(C_D\ v)$ aerodynamic resistance and r_c canopy resistance (Best, 1998):

$$r_c = min\left(10^{12}, 60/(f_S * f_e * f_T * f_M)\right) \tag{3.51}$$

with:

- solar radiation dependance:

$$f_S = 1.25\ R\downarrow_{SW}\ /(R\downarrow_{SW} + 250) \tag{3.52}$$

- vapor pressure deficit dependance:

$$f_e = 1 - (e_s(T_s)\ x - e_s(T_a)\ U_r)/40 \tag{3.53}$$

with U_r air relative humidity.

- temperature dependance:

$$f_T = (T_a - 0)(50 - T_a)/625 \tag{3.54}$$

if T_a is $> 50^oC$ or $< 0^oC$, $f_T = 10^{-12}$.

- water content dependance:

$$f_M = \begin{cases} 1 & \text{if } sat \geq 0.5 \\ 2 \cdot sat & \text{if } sat < 0.5 \end{cases} \tag{3.55}$$

3.4.5 Soil Heat Flux

The soil heat flux G is expressed as a function of the soil temperature T_s and is integrated with a finite-difference implicit scheme (Crank-Nicolson's method) on an arbitrary N soil layer (Incropera et al., 1994).

The soil is considered as a homogeneous means with specific heat c_s $[J/(kg\ K)]$, bulk density ρ_s $[kg/m^3]$ and thermic conductivity λ_s $[W/(K\ m)]$. These are constant with respect to the depth, but variable with the soil water content according to 3.56.

$$\begin{array}{ll} \lambda_d & = \rho_{sd}\ c_{sd}\ k_{sd} \\ c_s & = (c_{sd}\ \rho_{sd} + sat\ por\ c_w\ \rho_w)/(\rho_s + sat\ por\ \rho_w) \\ \rho_s & = \rho_{sd} + sat\ por\ \rho_w \\ k_s & = \frac{\lambda_d}{c_s\ \rho_s}\left(1 + 8(sat\ por)^{(1/3)}\right) \end{array} \tag{3.56}$$

where the index $_d$ indicates dry soil and the index $_w$ refers to water, c $[J/(kgK)]$ is the specific heat, λ $[W/m]$ the thermic conductivity , k $[m^2/s]$ the thermic diffusivity, $\rho[kg/m^3]$ the density, sat the saturation and por the porosity.

The soil depth is divided in a number of variable layers, depending on the precision requested in the computation.

The layer thickness increases with depth (Best, 1998) according to an exponential relation: the first layer is about 5 cm deep (to estimate the surface flux with a better precision) and the last layer is at a depth of 1 m (to avoid daily temperatures variations). The depth z_i of the layer i is given by the relation:

$$z_i = 0.013exp\left(4.35\frac{i}{N}\right) \tag{3.57}$$

where N is the number of layers.

At each iteration (i) the soil temperature is determined for the next instant ($i+1$), which satisfies the energy balance in the intermediate instant ($i + \frac{1}{2}$):

$$G(T_s^{i+\frac{1}{2}}) = R_n(T_s^{i+\frac{1}{2}}) - H(T_s^{i+\frac{1}{2}}) - \lambda ET(T_s^{i+\frac{1}{2}}) - \frac{\Delta E(T_s^{i+\frac{1}{2}})}{\Delta t} \tag{3.58}$$

The energy balance for the first soil layer between the surface and the depth d_1 in the instant $i + \frac{1}{2}$ is given by (see fig. 3.1):

$$G(T_s)^{i+\frac{1}{2}} + \frac{\lambda_s}{d_1}(T_1^{i+\frac{1}{2}} - T_s^{i+\frac{1}{2}}) = \rho_s c_s \frac{d_1}{2}\frac{T_s^{i+1} - T_s^i}{\Delta t} \tag{3.59}$$

while for a generic layer n with thickness d_n:

$$-\frac{\lambda_s}{d_n}(T_n^{i+\frac{1}{2}} - T_{n-1}^{i+\frac{1}{2}}) + \frac{\lambda_s}{d_{n+1}}(T_{n+1}^{i+\frac{1}{2}} - T_n^{i+\frac{1}{2}}) = \rho_s c_s \frac{d_n + d_{n+1}}{2} \frac{T_n^{i+1} - T_n^i}{\Delta t} \quad (3.60)$$

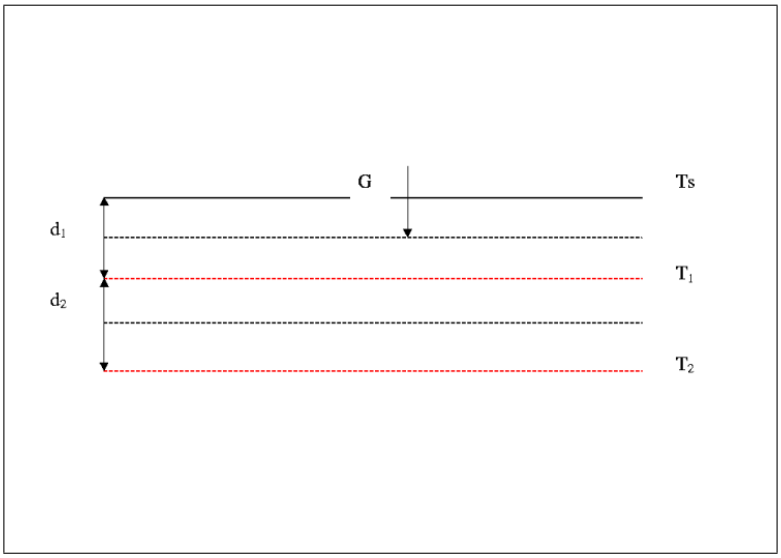

Figure 3.1: *Soil heat flux numerical scheme.*

At each integration time step, the program calculates a new value for the canopy intercepted water W_r and for the soil water content. The water necessary to the evaporation is supplied firstly by the surface water available (if it is present), secondly by the upper unsaturated layer, lastly by the the lower saturated layer (if the water demand is greater than the amount of water available in the upper layer). The energy flux of latent heat is converted into mass flux using the relation:

$$ET[mm] = 1000 \frac{ET[W/m^2]}{\lambda \, \rho_w} \quad (3.61)$$

The upper boundary condition, at the soil surface, is given by the atmospheric forcing, while the lower boundary condition, at a depth of about 1 m, is given by a known temperature T_{sn}. This temperature is the analytical solution for the annual cycle, assuming that it has a sinusoidal behaviour. Actually, at a depth of 1 m, the diurnal cycle of temperature is negligible, but the annual cycle is still significant. Therefore, the sinusoidal solution T_n at a depth of Δz is given by:

$$T_{sn} = T_{med.ann} + \frac{\Delta T_{ann}}{2} \cdot \exp(-\gamma_s \, \Delta z) \sin(\omega_{ann}(gg - \delta_{gg}) \cdot 24 - \gamma \, \Delta z) \quad (3.62)$$

where $\gamma_s = \sqrt{\omega_{ann}/(2 \cdot k_s \cdot 3600)}$, with $k_s \; [m^2/s]$ soil thermic conductivity, $\omega_{ann} = 0.0007167 \; [rad/h]$ angular earth speed, and $\delta_{gg} = 109 \; gg$ phase displacement.

The mean annual temperature $T_{med.ann}$ and the annual temperature range T_{ann} are determined by using a mobile means with a period of 7 days on the air temperature data.

The initial condition is given by a linear temperature variation ranging from the air temperature to the lower boundary condition temperature. After about one day of simulation,the results obtained are almost independent from the initial condition after about 1 day of simulation.

3.4.6 Unknown Parameters

The unknown parameters in the energy balance model are also:

- Albedo a.
- Soil longwave emissivity ϵ_s.
- Momentum roughness length z_0 and heat roughness length z_T.
- Soil bulk density ρ_s, soil specific heat c_s thermic conductivity λ_s.
- Soil saturation sat.

All those parameters have to be given as input, except the soil saturation, which is determined by the hydrological part of the model.

3.5 The hydrologically active soil thickness

The topography influences the distribution of the soil water content inside a catchment and plays a pivotal role in the hydrologic accounting, which the $\mathrm{GEO_{TOP}}$ model (*Bertoldi and Rigon*, 2002; *Rigon et al*, 2002) can investigate with precision.

The surface runoffs celerity (depending on the square root of the local slope) and the hypodermic runoffs (proportional to the local slope) are some of the main aspects controlled by topography. Yet two more elements at least, influenced by topography, can modify the hydrologic accounting in a significant way, i.e. the hydrologically active soil thickness, and the channel net extension. *Stocker* (1998), developing *Hiemsath et al*'s model (1997), suggested that in condition of stationary balance between soil production and erosion, the soil thickness h is obtained though the following expression, valid for the convex zones ($\nabla^2 z$<0):

$$h_s = -\frac{1}{m} \ln \left[-\frac{k \cdot \nabla^2 z}{P_0 \cdot \frac{\rho_r}{\rho s}} \right] = \frac{1}{m} \left[\ln \left(\nabla^2 z_{crit} \right) - \ln(-\nabla^2 z \right] \tag{3.63}$$

in which $\nabla^2 z_{crit}$ (<0) is the critic curvature, to which the rock outcrops correspond, P_0 the soil production at the initial instant, $m$the inverse of the soil production for unit time, ρ_r the rock's porosity and ρ_s the soil's, k a diffusivity.

On the other hand, in the concave zones the soil thickness depends on the basin's geologic history.

3.6 Channel network extraction

Prosser and Abermethy (1996) suggested that the canals incision takes place only if the stress tangent to the bottom exceeds a critical threshold value (τ_{lim}), which can be expressed according to the relations:

$$\tau = \alpha\sqrt{S} \cdot \nabla z > \tau_{\lim} \tag{3.64}$$

$$\nabla^2 z > 0 \tag{3.65}$$

in which S is the area upriver from the point considered, ∇z is the local slope and α is the adequate coefficient which describes the runoff concentration on the versants in rivulets inferior in largeness to the basin's grid resolution. If a point is classified as river, all downstream points have to be classified in the same way.

Both relations 3.63 and 3.64 state that the increasing-slope basins have less soil available on the versants (therefore they tend to become saturated earlier), and they have, if the lithology is the same, a superior drainage density.

3.7 Runoff Generation

The process of runoff generation including infiltration and lateral distribution in the hillslopes is described with more in detail in Pegoretti (1999). Here, only a brief report is given.

The process of infiltration is described through a "bucket model". If the rain intensity is greater than the saturated infiltration velocity, there is infiltration excess runoff, otherwise the amount of water in the upper unsaturated layer increases. The infiltration velocity is assumed to be constant in the whole soil layer.

If the water amount in the unsaturated upper layer is greater than the field capacity (fixed as a saturation of 10%), the vertical water movement as far as the bedrock is possible. When the water reaches the bedrock, which is assumed to be impermeable, a saturated lower layer begins to form. The water table elevation depends on the mass balance between vertical fluxes (infiltration and evaporation) and lateral redistribution according to the local water table slope. If the saturated layer reaches the surface, saturation excess runoff begins.

3.7.1 Surface Flow

The surface runoff for contour units is given using:

$$F_s = v_s \, h \tag{3.66}$$

where Fs is the surface runoff, h surface water depht, v_s the velocity, calculated with a uniform-motion relationship;

$$v = C \, h \, i^{0.5} \tag{3.67}$$

where C is Chezy's parameter and i the slope. C is assumed to be a stochastic variable with given mean and variance.

3.7.2 Subsurface Flow

The subsurface flow is described coupling the continuity equation to Darcy's equation.

The lateral water distribution is related to the local water table slope:

$$v = k\frac{\partial h}{\partial L} \tag{3.68}$$

Where h is piezometric elevation.

Therefore, the maximum water flow depends not only on permeability and slope, but also on soil depth.

The continuity equation is written in each cell as:

$$\frac{\partial}{\partial t}\int_V \theta(y,t)dV + \int_s q \cdot n \, dS = 0 \tag{3.69}$$

where $\theta(y,t)$ is the soil water content at time i, q is the specific flux through the surface dS with normal n. The second part of the equation represents the net flux through the contour dS and comes from the algebric sum of net precipitation $P(t)$, subsurface flow $Rs(t)$ and evapotranspiration $ET(t)$. For a single pixel i, the equation is:

$$\theta_i(t) = \theta_i(t-1) + q_i(t)\delta A + T\left(\sum_{j\in N} W_{ij}\tan\beta_j\delta x - \tan\beta_k\delta x\right) - E_i(t) \tag{3.70}$$

$$W_{ij} = \begin{cases} 1 & \text{if } i \rightarrow j \\ 0 & \text{otherwise} \end{cases} \tag{3.71}$$

where dA is the pixel area, β is the slope, N are the eight pixel placed around the element i, k is the element where i drains, dy the pixel side and T the hydraulic soil conductivity:

$$T = k\, h \tag{3.72}$$

with k mean hydraulic conductivity (constant across the basin) h soil depth (varying with the elevation curvature).

3.7.3 Coupling between hillslope and River Network

Firstly, the distance from the closure section of the farthest point across the basin is calculated, secondly this distance is divided in a large number of intervals. The water coming from the hillslopes flows into the river network at a different distance from the outlet, therefore it is assigned at different intervals. In this way a dynamic width function is created: it represents the whole flow entering the river network at every distance from the outlet. All the water flux going in the river network at the same distance from the outlet is considered in an aggregate way (see flg. 4.6 and 4.5).

3.8 Water movement in the River Network

The movement in the channel network is described in an aggregate way, by using a constant celerity in the whole basin (Bathurst, 1993).

The motion inside the channels is described by the parabolic solution of the De Saint Venant equations, by using a constant celerity in the whole network as proposed in (*Rinaldo et al.*, 1991) and globally described by the:

$$Q(t) = \int_0^t \int_0^L \frac{xW(\tau,x)}{\sqrt{4\pi D(t-\tau)^3}} \exp\left[-\frac{(x-u(t-\tau))^2}{4D(t-\tau)}\right] d\tau \cdot dx \quad {}^{(1)} \tag{3.73}$$

where $Q(t)$ is the discharge at the basin's closing section , $W(t,x)$ is the inflow of the water coming from the hillsides into the channel network at a distance x from the outlet

and at a time t, u an opportune mean celerity, D a hydrodynamic dispersion coefficient, L the maximum distance from the outlet measured along the network. The values of the celerity u and of the diffusivity D are to be determined with a calibration from the experimental outflow data.

Chapter 4

Geomorphological Analysis

The program performs several geomorphological analyses of topography. Several intermediate matrixes are then created, written in the output files listed in the paragraph 8.8.1.

4.1 Pit cleaning

The DEM often has a non-coherent drainage direction network, due to the presence of pits or areas without outlets. These can be due to errors in the DEM or can be real physical features (for example pit are frequent in carsick ares or in quite flat zones).

Before running the program, it is necessary to have a DEM with no pits. In the beginning, the program runs automatically a pit cleaning tool.

4.2 Drainage directions

Matrix with *Drainage directions*: pixels are classified according to the D8 rule, with codes from 1 to 8 (see figure 4.1) (Rodriguez-Iturbe and Rinaldo, 1997). If the pixel is coded as channel the code is 19, if it is lake the code is 11, if it is outside the basin it is 9 (Cozzini, 1999).

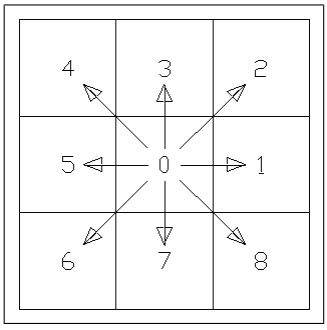

Figure 4.1: *Drainage direction classification used by the program.*

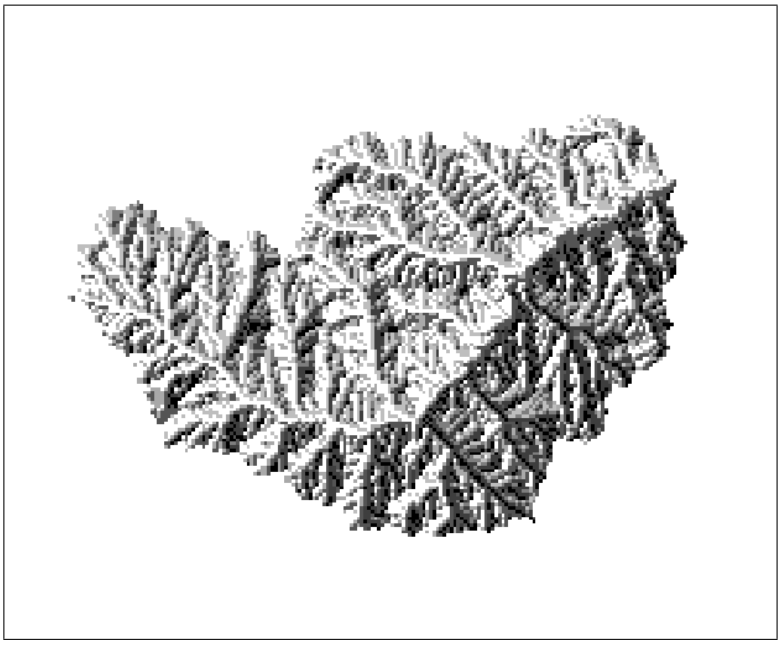

Figure 4.2: *Example of drainage direction map for the Little Washita basin, OK, USA.*

4.3 Up slope catchment area

Matrix with *upslope catchment area*: it contains the upslope contributing area of each pixel.

4.4 Laplacian

Matrix with the *laplacian* ($\nabla^2 z$) of the topography: this information is used for the soil thickness model, for the water content distribution, for the shadow map. A map with conventional value - 1 for convergent zones ($\nabla^2 z > 0$), 0 for divergent zones ($\nabla^2 z < 0$) is also calculated -.

4.5 River network

Matrix with the *river network*: it is automatically extracted form the DEM. The extent of the network is controlled by the parameter τ_{lim} (to set in the routing file), as explained in par. 3.6.

The river network extent is an important parameter to control the flood wave formation and the drainage velocity in the basin (Bertoldi, 2002).

4.6 Distance from outlet

Matrix with the *distance of each point from the basin outlet*: it contains the distance (positive values) of a channel pixel from the outlet and the distance (negative values) of a hillslope pixel from the nearest channel pixel.

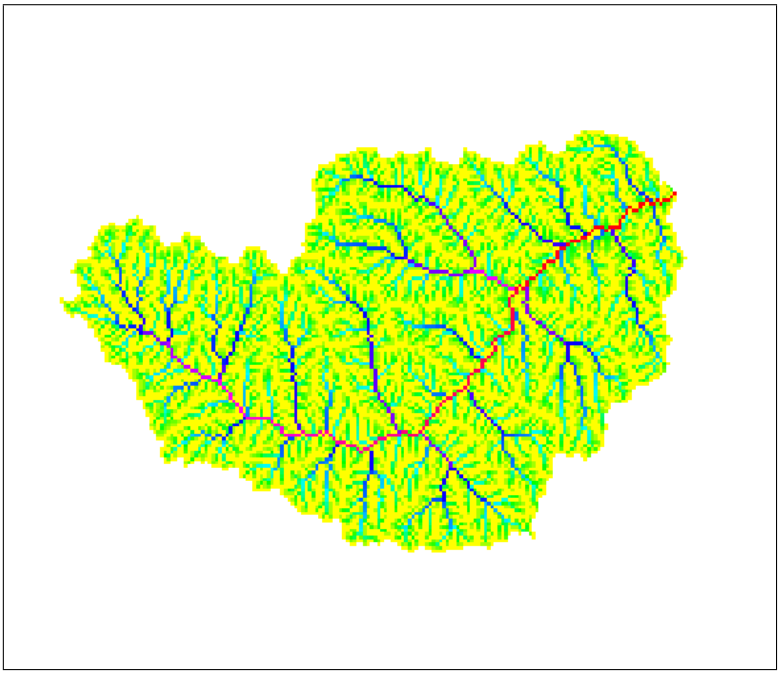

Figure 4.3: *Example of upslope contributing area map for the Little Washita basin - OK, USA.*

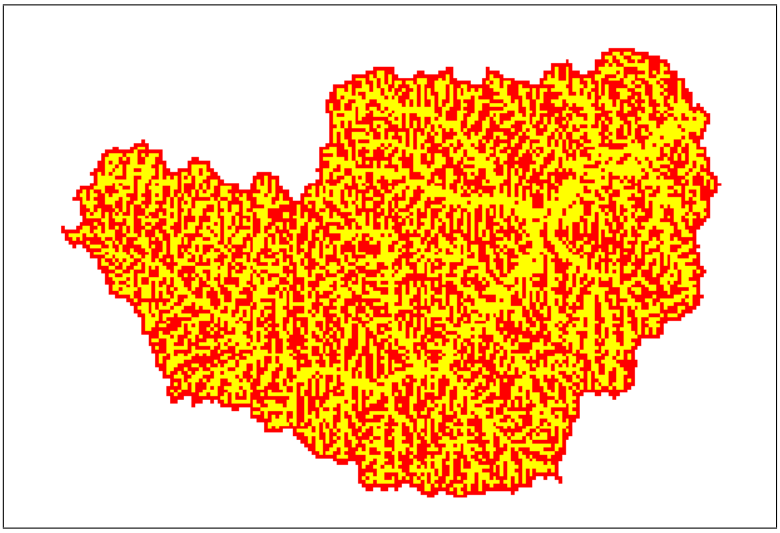

Figure 4.4: *Example of curvature map for the Little Washita basin - OK, USA. In red divergent areas, in yellow convergent ones.*

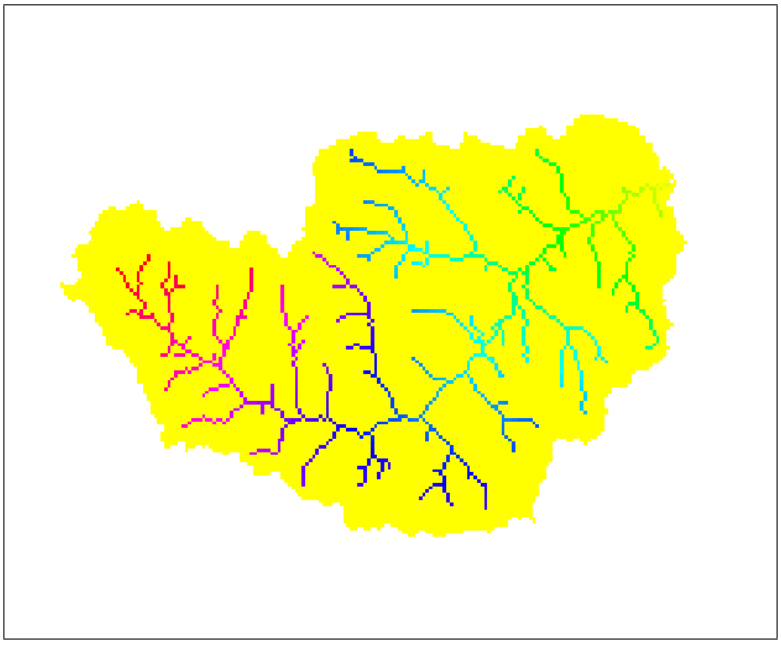

Figure 4.5: *Example of river network map for the Little Washita basin OK, USA.*

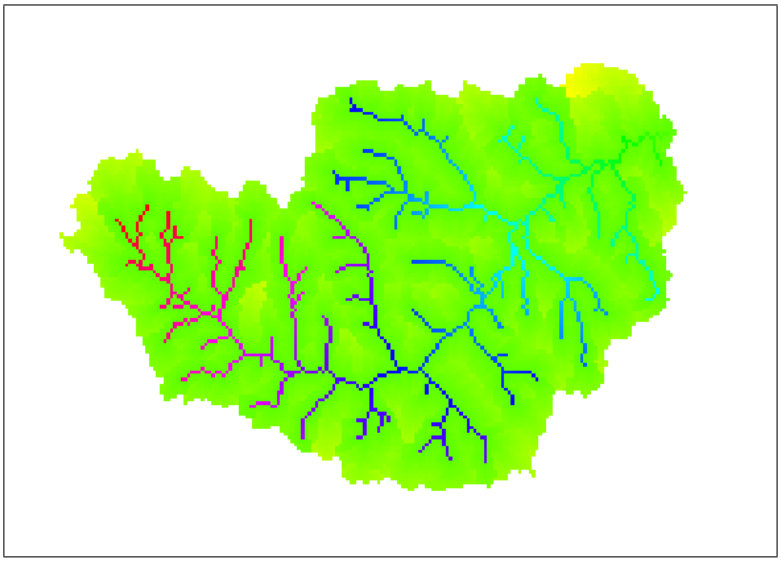

Figure 4.6: *Example of distance from outlet map for the Little Washita basin OK, USA. Color range is from yellow (maximum distance from river networks), to green (along the river network), to red (maximum distance in the river network).*

4.7 Soil thickness

Matrix with the *soil thickness*: if experimental data are not available, it is calculated using a soil production model, as explained in the paragraph 3.5. The parameters of the equation 3.63 m, P_0, ρ_r, ρ_s, k (constant for the whole basin and inferred from literatures values (Heimsath et al., 1997)) are indicated in the paragraph 7.6.

The saturated area distribution in hillslopes is controlled both by the upslope catchment area, and by the soil thickness. This last factor is also important to control the maximum amount of water stored by the catchment and also the maximum amount of evaporation. They thickness of the soils controls also the probability of Dunnian flow occurrence: if the soil is shallow, the saturation of the soils column occurs more quickly.

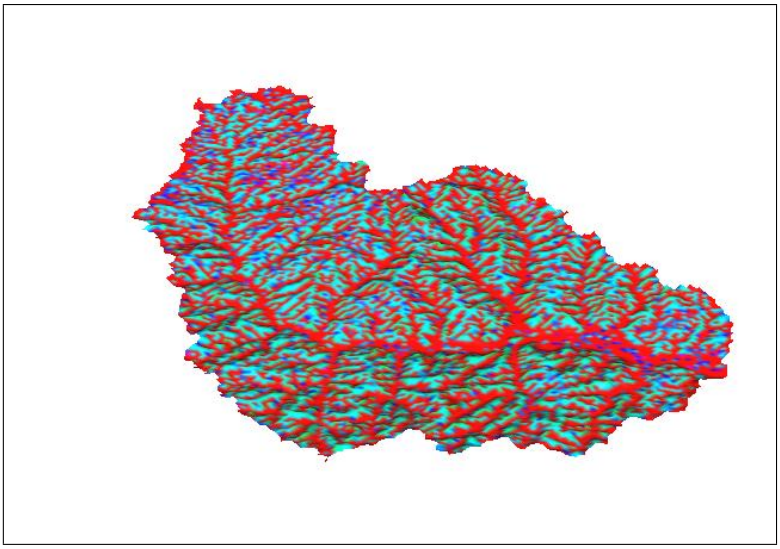

Figure 4.7: *Example of soil thickness map for the Little Washita basin OK, USA. In convergent areas we have fixed soil thickness (red color), in divergent areas the thickness is decreasing.*

4.8 Water storage volume

Matrix with *water storage volume* in the basin: the void volume V_v $[m^3]$ is given by:

$$V_v = h_s \cdot A \cdot \theta_s \tag{4.1}$$

where h_s is the soil thickness, A is the pixels area, θ_s is the porosity, the latter given by:

$$\theta_s = 1 - \rho_s/\rho_r \tag{4.2}$$

4.9 Gradients

Matrix with *gradients*: gradients are computed as the difference between the elevation of a pixel and the pixel downstream according to the steepest descent divided by the

distance of the center of the two pixels. Gradients are needed for the calculation of surface and subsurface flows.

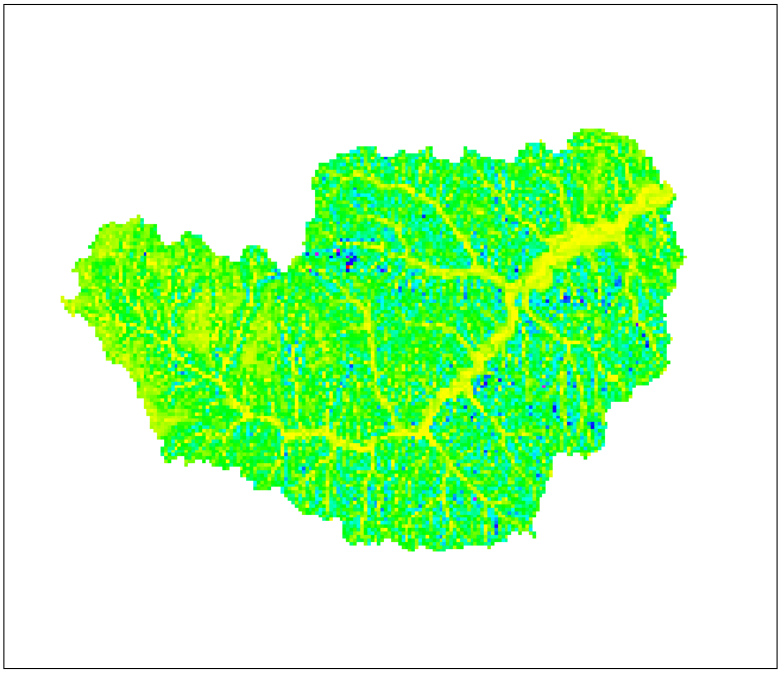

Figure 4.8: *Example of gradients map for the Little Washita basin (OK, USA). Color range is from yellow (minimum value), to red (maximum value).*

4.10 Slope and Aspect

Matrixes with *slope* and *aspect*: they are useful for the calculation of the incident solar radiation. The convection used for the aspect is: 0^o N, hourly direction.

If we call:

$$a = \arctan(\frac{\partial z}{\partial y}) \tag{4.3}$$

and

$$b = \arctan(\frac{\partial z}{\partial x}) \tag{4.4}$$

with z elevation, y north - south direction, x east - west direction, the slope ϑ and the aspect φ are given by:

$$\vartheta = \arccos(\cos|a| \cdot \cos|b|) \tag{4.5}$$

$$\varphi = \arccos(\frac{\sin|a| \cdot \cos|b|}{\sqrt{1-(\cos a)^2(\cos b)^2}}) \tag{4.6}$$

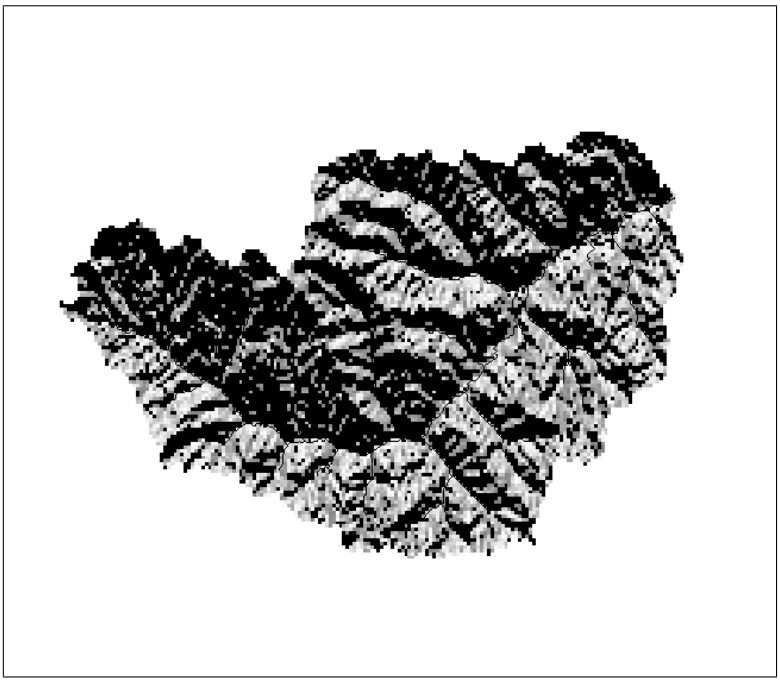

Figure 4.9: *Example of aspect map for the Little Washita basin (OK, USA).*

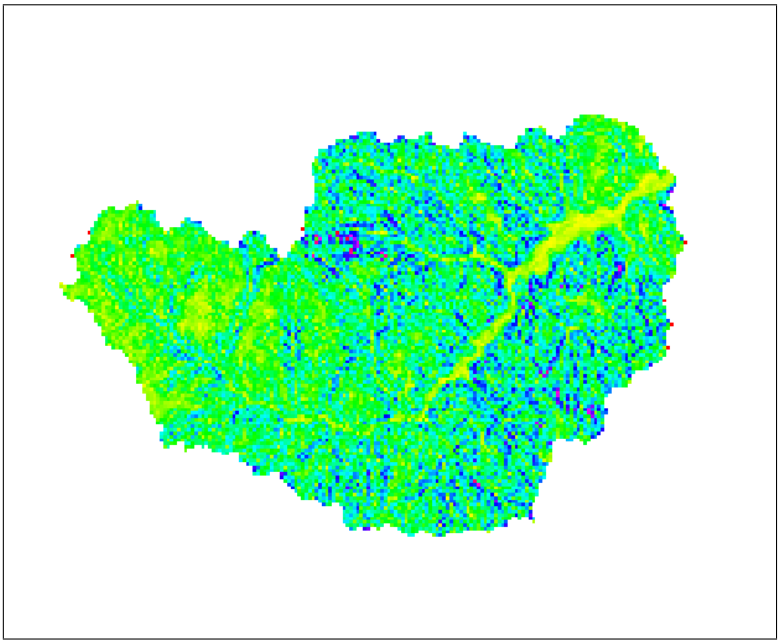

Figure 4.10: *Example of slope map for the Little Washita basin (OK, USA). Color range is from yellow (minimum value), to red (maximum value).*

4.11 Water content

As explained in the paragraph 3.7, the water volume [m^3] in each pixel is divided in three layers (see figure 7.7):

1. Vol_{sur} the *surface layer*;
2. Vol_{uns} the *unsatured upper layer*;
3. Vol_{sat} the *lower satured layer*.

The program stores the information in three matrixes. The sum of these volumes gives the total water volume in the basin. The soil saturation s is also given by the equation 3.46.

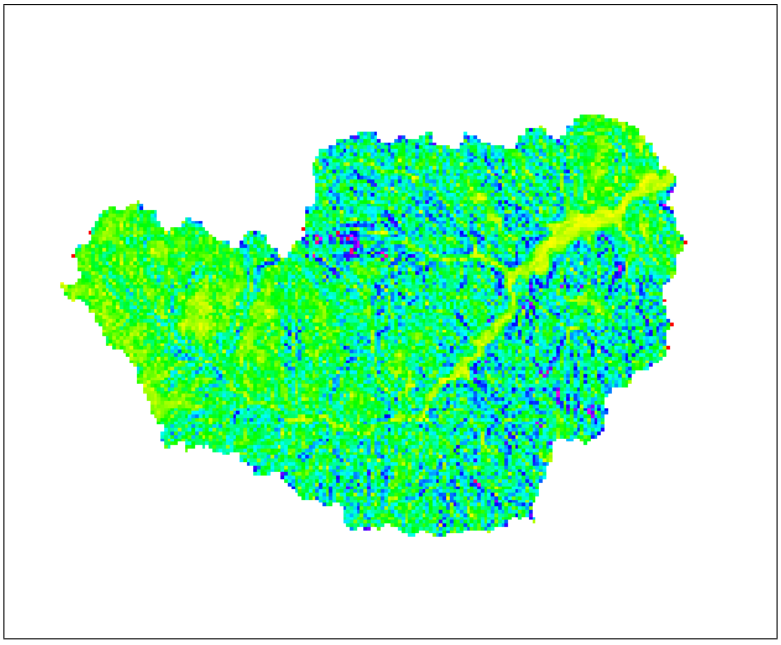

Figure 4.11: *Example of distribution of the saturated water coneten the Little Washita basin (OK, USA). Color range is from yellow (minimum value), to red (maximum value).*

4.12 Canopy cover fraction and canopy height

The program, using the information about the *Land Cover Map* and the *Land Cover Classification* (see par. 7.7 and figure 7.6), creates two matrixes with the *canopy cover fraction* (0 - 1) and the *canopy height*. The first one is used to calculate the canopies water interception and the partition between vegetation and bare ground evaporation, the second one is used to estimate the roughness for the air turbulence parameterization.

Chapter 5

Data requirements for the model *GEOTOP*

1. **Meteorological data strictly necessary to run the model**

   At least 1 station with **hourly** data. The more stations are available, the better it is.

   - Air temperature T_a.
   - Relative humidity R_h or air water content or air vapor pressure or dew point.
   - Wind speed v.
   - Shortwave radiation $R\downarrow_{SW}$.
   - Pressure P_a.
   - Precipitation P.

2. **Recommended data to run the model with more precision**

   - Longwave radiation $R\downarrow_{LW}$.
   - Diffuse shortwave radiation $R\downarrow_{SW\ diff}$.
   - Net radiation R_n.
   - Sky fraction covered by clouds.
   - Snow precipitation.

3. **Data useful for a *point* validation of the model**.

   It is useful to have measurements of all term of the energy balance components (net radiation Rn, soil heat flux G, sensible heat flux H, latent heat flux ET), in one point at least.

   - **Soil heat flux** G.

     The soil heat flux can be measured by using a **heat flux plate** or by measuring the **soil temperature profile**, the soil bulk density, the fractions of clay, loam, gravel, rock, organic matter and the volumetric water content (see hereafter).

- **Turbulent fluxes** H, ET.

  The turbulent fluxes can be measured by using an **eddy covariance system** (sonic anemometer for H, KH20 hygrometer for ET), or by using a **bowen ratio system** (air temperature and dew point at two different heights).

As an alternative, the **potential evaporation** EP can be directly measured by using a **lysimeter**.

It is also useful to measure the **soil moisture**. The soil water content can be measured by using a **time domain reflectometer** (TDR) or by using an **electrical capacitance** sensor. It would be very useful to have a net of TDR on a hill side, as a probe zone.

It may also be useful to measure the **soil water matrix potential**, by using electrical resistance methods, and the **water table depth**, by using piezometers.

All these methods require calibration, with some soil samples and with the knowledge of the soil bulk density, the soil texture (fractions of clay, loam, gravel, rock, organic matter) and the volumetric water content (see later).

For the calibration of the **snow melt** model, **snow depht** and **snow density** are needed.

4. **Distributed data strictly necessary to run the model**

   - **Digital Elevation Model (DEM)** of the basin.
   - **Land use map** of the basin. At least a classification with urban, forest, bare soil, agricolture, pasture.

5. **Other distributed data useful to run the model**

   The model needs the following information, but, if it is not available, values taken from literature are used.

   - **Soil texture**: fraction of rock, gravel, sand, loam, clay, organic matter, bulk density.
   - **Soil depth**, how deep is the bedrock.
   - Soil **hydraulic conductivity**, information regarding how permeable the bedrock is (fractures, carsick formations).
   - Surface **roughness**, including the height of obstacles on the surface (buildings, vegetation).
   - Information regarding **vegetation** is essentially of three types: **vegetation density** (fraction of vegetation cover and Leaf Area index (LAI)), **seasonal variation** of vegetation (Normalized Vegetation Deviation Index (NVDI)), **vegetation height**. These indexes are often available with coarse resolution in global data sets.

6. **Distributed data useful to validate the model**

   Remote sensing images:

   - **Brightness temperature**.
   - Surface **Soil moisture**.
   - **Albedo**.

- **Snow cover** distribution.

Distributed measurements in different points across the basin of:

- Soil volumetric water content.
- Water table depth.
- Meteorological variables in different point across the basin at different elevations and aspects.

Chapter 6

Programs structure

The program GEOTOP is written in C language, using the $FluidTurtle$ (Rigon, 2001) libraries.

The code is organized in a first part, where input data are read and some preprocessing is done (some geomorphological analysis, like drainage direction calculation and river network extraction), and in a second part, where are calculated the mass and energy fluxes each time step.

The most important parts of the program are handling:

1. The calculation from the DEM of slope, aspect, curvature, soil depth, drainage directions, cumulated area, river network;
2. The distribution of precipitation inside the basin;
3. The relationship between elevation and air temperature and pressure;
4. The calculation of the shadows;
5. The relationship between solar radiation, time, slope and aspect;
6. The surface energy balance;
7. The mass balance in each cell calculating vertical and lateral water flows.
8. Modelling surface and subsurface flow in the hillsides;
9. Coupling between hillsides flow and channel network;
10. The water movement in the channel network;

The structure of GEOTOP can be summarized in the flow chart 6.1.

6.1 Programs files and subroutines

The code is divided in different files.

***geotop.c*:** It contains the main program.

geotop_inputs.c It contains some subroutines for the Input/Output of data and for the allocations/deallocations of some internal matrices and structures.

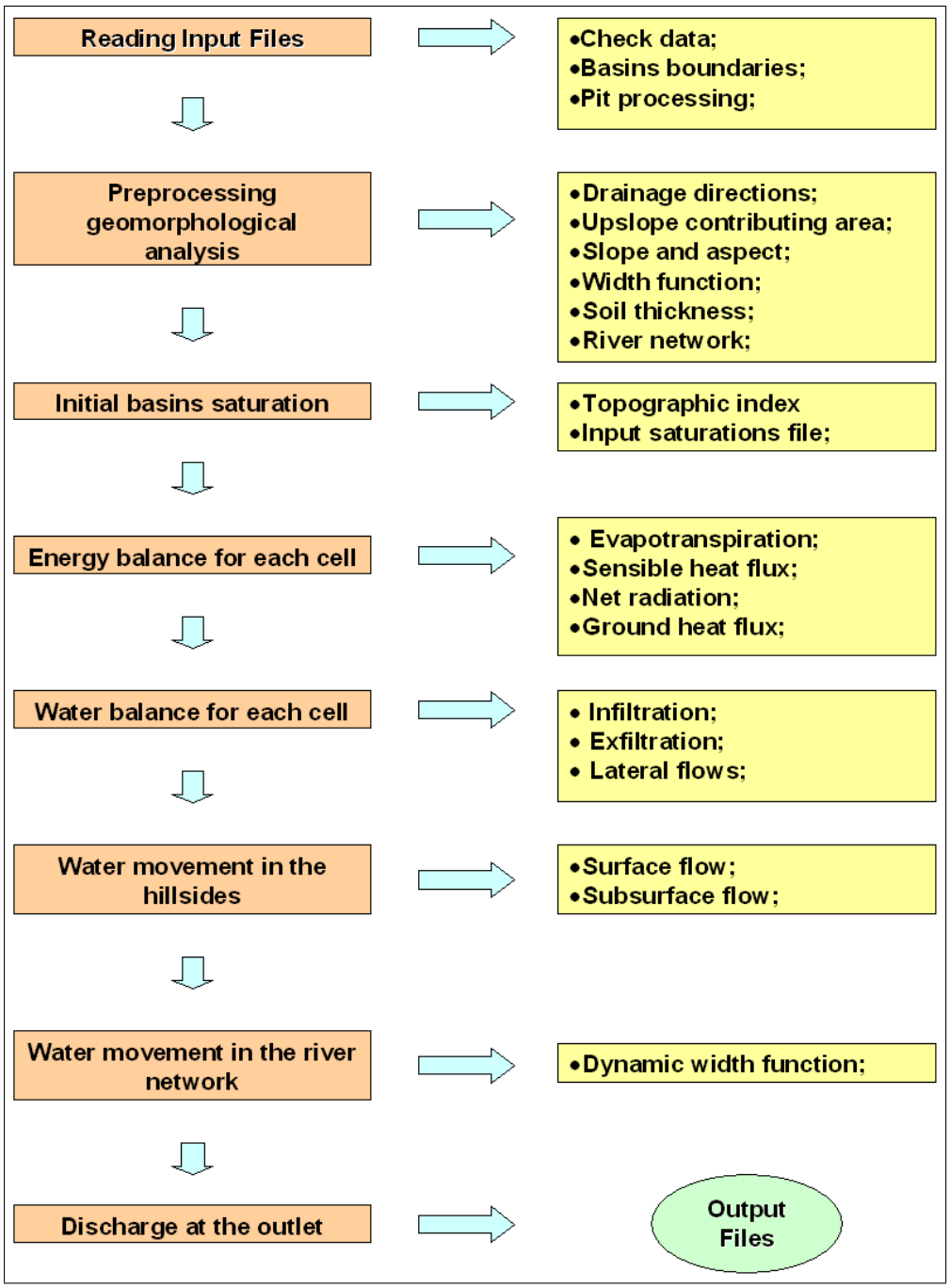

Figure 6.1: *Flow chart of the program GEOTOP.*

- $deallocatestruct$
- $evapo\_initialization$
- $geo\_initialization$
- get_Albedo
- $get\_classification\_soil$
- $get\_meteorological\_inputs$
- get_snow
- get_soil_inputs
- $get\_topografic\_inputs$
- $get\_turtleinit$
- get_synop_inputs
- get_Volume
- $print\_output\_stazione$
- $roughness\_initialization$
- $volume\_initialization$
- $write\_out\_matr\_file$

***geotoplib.c*:** It contains various subroutines, specific developed for the program GEOTOP.

- $altezza\_scabrezza$
- $estremi$
- $Orizzonte$
- $rout\_evapo$
- $rout\_fl$
- $topogr\_ind$
- $volume$

***hydrology.c*:** It contains various subroutines of hydrological interest.

- $cond\_cont$
- $effective$
- $evapo\_punt$
- $geomodel$
- $Iniz\_Bil\_En$
- $interpola\_meteo$
- $layer$
- $maxtime$
- $pioggia$
- $pioggia\_distr$
- $Pressione\_nuova$
- $previsione$

- $radiazione\_nuova$
- $scabrezza$
- $shadow\_n$
- $responce$
- $temp\_med$
- $temp\_med\_annuale$
- $Temperatura\_nuova$

***geomorphology.c*:** It contains some subroutines with the geomorphological analysis of the basin.

- $area$
- $aspetto$
- $gradients$
- $nablaquadro$
- $nablaquadro\_mask$
- $pits\_filler$
- $profondita$

***networks.c*:** It contains some subroutines with the river network analysis.

- $drainagedirections$
- $drainagedirections\_modify$
- $go\_downstream$
- $hillslopes\_channels\_outletdistance$
- $is\_ontheborder$
- $select\_hillslopes$
- tca

***snow.c*:** It contains some subroutine for the snowmelt module.

- $part\_snow$
- run_albedo

***geo_statistic.c*:** It contains some subroutine for the the interpolation of spatial distributed input data.

- $gamma1$
- $ordi\_kriging$
- $variogramma$

***FluidTutle Libraries*:** It contains, in several files, the FluidTurtle libraries, which allow a easier process for reading and writing data files and for programming with arrays than with standard C. For a detailed description of the FluidTurtle libraries, see Rigon (2000).

6.2 Programs tree

The code is organized in several parts. Here are reported only all the subroutines used by the program, in the order used in the code. For a detailed explanation of the subroutines, see chapter 6.

- Main program.
- Read input parameters. The parameters are read from the file *geotop.inpts*
- Read input files. The contents of those files are described with more detail in the previous chapter. Those files are read in the following order:

  Input 1 The file with the DEM of the basin.

  Input 2 The file with the sky view factor of the basin.

  Input 3 The file with the rain data.

  Input 4 The file with the meteorological data.

  Input 5 The file with soil parameters.

  Input 6 The file with the land cover map of the basin.

  Input 7 The file with the initial soil moisture map of the basin (optional).

  Input 8 The file with the cloud cover data.

  Input 9 The file with the albedo map of the basin.

  Input 10 The file with the proprieties of each land cover class.

  Input 11 The file with the initial snow water content map of the basin.

  Not all input files are necessary for the simulations: if some data are unavailable, the user can specify in the parameter file *geo_top.inpts* that some files are skipped. This is possible for the *Input 7, Input 8, Input 11*.

- Create output files. The contents of those files are described with more detail in the previous chapter. Those files are created in the following order:

  Output 1 The file with output hydrograph in the closure section of the basin.

  Output 2 The file with total flow going in to the lakes (if they exist).

  Output 3 The file with the final soil moisture map of the basin.

  Output 4 The file with mean values of different quantities at each timestep for the whole basin.

  Output 5 The file with values of different quantities in a particular point, specified in the input parameters.

  Output 6 The file with mean values of different quantities for the whole basin, given as temporal mean on specified timestep.

  Output 7 The file with some simulations controls.

- Call $rout\_fl$ in $geotoplib.c$. This subroutine call several other commands, which are doing several geomorphological analysis. $rout\_fl$ calls:

  – $pits\_filler$ in $geomorphology.c$: it fills the pit eventually present in the DTM.

  - $nablaquadro$ in $geomorphology.c$: it calculates the elevations second derivative.
  - $gradients$ in $geomorphology.c$: it calculates the elevations gradient.
  - $profondita$ in $geomorphology.c$: it calculates the soil depth, according the eq. 3.63.
  - $drainagedirections\_modify$ in $networks.c$: it calculates the drainage direction, according the $D8$ rule.
  - $select\_hillslopes$ in $networks.c$: it uses curvatures and contributing areas to extract channels from drainage directions.
  - $hillslopes\_channels\_outletdistance$ in $networks.c$: it returns the distance from the outlet of hillslopes and channels cells, separately.
  - tca in $networks.c$: it returns the total cumulated area above each cell.

- Call $rout\_evapo$ in $geotoplib.c$. This subroutine call several other commands, which are doing several calculation, useful for prepare the data for the evapotranspiration part. $rout\_evapo$ calls:
  - $nablaquadro\_mask$ in $geomorphology.c$: it distingue between convergent and divergent cells.
  - $area$ in $geomorphology.c$: it returns the area of the basin, considering the slope.
  - $aspetto$ in $geomorphology.c$: returns slope and aspect.
  - $altezza\_scabrezza$ in $geotoplib.c$: returns the vegetation height and density matrices, using the land cover information.
- Call $scabrezza$ in $hydrology.c$. This subroutine, from the land cover data, calculates the roughness map for the basin.
- Call $temp\_med\_annuale$ in $hydrolgy.c$. This subroutine, from the air temperature data, calculates mean annual air temperature.
- Call $estremi$ in $geotoplib.c$. This subroutine calculates the minimum and the maximum value of width function, calculated in $rout\_fl$.
- Call $volume$ in $geotoplib.c$. This subroutine calculates the distance of the channel pixel from the hillsides.
- Call $ordi\_kriging$ in $geostatistic.c$. This subroutine calculates the coefficients for the interpolation of the precipitation, made with the Ordinary Kriging method.
- Call max_time in $hydrology.c$. This subroutine calculates the maximum time used by the water flow to go in the river network.
- Call $topogr\_ind$ in $geotoplib.c$. This subroutine calculates, if input data are unavailable, the initial soil moisture content with the method of the topographic index.
- Call $layer$ in $hydrology.c$. This subroutine divides the soil depth in several layers for the calculation of the soil heat flux.

- Call $print\_output\_stazione$ in $geotop\_inputs.c$. This subroutine write several information about the actual simulation on the $Output5$ file.
- Begin of the temporal cycle of the simulations.
- Call $pioggia\_distr$ in $hydrology.c$. This subroutine calculates the matrix with the actual rain amount in each pixel from the rain data (***input 3 file***) and from the coefficient calculated in $ordi\_kriging$.
- Call $Iniz\_Bil\_En$ in $hydrology.c$. This subroutine calculates several important quantities depending on time, used later for the energy balance calculation. It calls the following subroutines:
  - $shadow\_n$ in $hydrology.c$: it returns cells with shadow at the given time.
  - $interpola\_meteo$ in $hydrology.c$: it returns the meteorological inputs at given time.
  - $Temperatura\_nuova$ in $hydrology.c$: it returns the air temperature matrix.
  - $Pressione\_nuova$ in $hydrology.c$: it returns the air pressure matrix.
  - $radiazione\_nuova$ in $hydrology.c$: it returns the shortwave radiation matrix.
- Call $Part\_snow$ in $snow.c$. This subroutine separates solid from liquid precipitation, basing on the air temperature.
- Internal loop where for each pixel, in a iterative way, is solved the energy balance.
- Call $evapo\_punt$ in $hydrology.c$. This subroutine solves the energy balance for each pixel. It is called recursively until the soil temperature, which satisfy the energy balance, not change.
- End the energy balance loop.
- Call $geomodel$ in $hydrology.c$. This subroutine calculates the water balance for each pixel, taking in account the interactions between pixels and quantify the amount of the surface and of the subsurface flow. $geomodel$ calls the following subroutines:
  - $effective$ in $hydrology.c$: evaluates the actual soil water content.
  - $previsione$ in $hydrology.c$: check the subsurface flow.
  - $soilmoist$ in $hydrology.c$: it updates the soil water content.
- Call $responce$ in $hydrology.c$. This subroutine calculates the hydrological response of the whole catchment, using the output of $geomodel$ to determine the streamflow in to the channels.
- Check of the mass balance for the whole basin.
- Call $write\_out\_matr\_file$ in $geotop\_inputs.c$. This subroutines writes on files the matrices of several quantities. The values are temporal averages during a user established time step.
- End of the simulations temporal cycle.
- Write all output files.

6.3 Data files structure

All data files are **ascii** file in **FluidTurtle** format. This format can be easy read and written using the **FluidTurtle** C library (Rigon, ???).

All characters between `/**` and between `*/` are comments. They are not read by the program and you can write everything you want, except the carachter **:**, wich is reserved.

The expression `index{n}` indicates the number n of data blocks present in the file.

The data types used in **GEOTOP** are mainly **FluidTurtle** arrays or **FludiTurtle** matrices.

Arrays are defined as follow: index, data type, name, elements beween { }. Example:

```
1: float array header {15,15,0,0}
```

Matrices are declared with the same rule (index, data type, name, rows, columns), but without include the elements in brackets. Example:

```
2: long matrix data {2,3}
2 3 4
7 6 5
```

An example of DEM like data file is shown in figure (6.2).

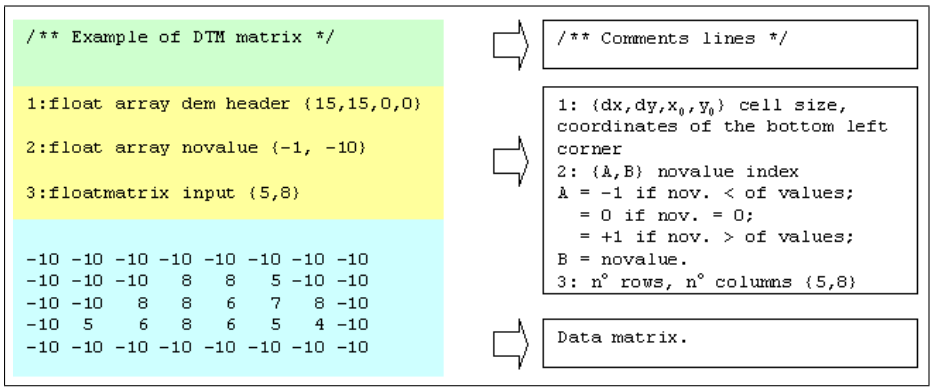

Figure 6.2: *Example of DEM GEOTOP inputfile.*

Chapter 7

Input Data Files

The program needs different input files. All files have to be in the same folder. This folder can be specified in a file, called `\$WorkingPath`. This file is in the same folder where the executable file is. The program reads the `\$WorkingPath` file and searches all input files in the given folder. All output files are also saved in the same folder. An example of the content of the file `\$WorkingPath` is the following:

```
C:\075\DATA\geotop\washita\
```

All parameters and input output file names list are contained in the routing file *geo_top.inpts*.

The input file are the following:

Routing file: file with input / output filenames and parameters *(File geo_top.inpts)*.

Input 1: the file with the DEM of the basin *(File Elevation)*.

Input 2: the file with the sky view factor of the basin *(File Sky)*.

Input 3: the file with the rain data *(File Data Rain)*.

Input 4: the file with the meteorological data *(File Data Meteo)*.

Input 5: the file with soil parameters *(File Data Soil)*.

Input 6: the file with the land cover map of the basin *(File Land cover map)*.

Input 7: the file with the initial soil moisture map of the basin (optional) (*File Soil Moisture*).

Input 8: the file with the cloud cover data *(File Cloud Cover)*.

Input 9: the file with the albedo map of the basin *(File Data Albedo)*.

Input 10: the file with the proprieties of each land cover class*(File Land cover classes)*.

Input 11; the file with the initial snow water content map of the basin *(File Snow Cover)*.

7.1 The Routing File

The *Routing File* is the program control file. It contains all input and output file names and the parameters needed by the program. All data are read by the program consequentially. The routing file has to have the standard name "*geo_top.inpts*" to be automatically recognized by the program. If the file is not present, the user can prompt all parameters from the command window.

The file is divided in two blocks:

1. String array input / output files.
2. Float array parameters:
   - **a)** Control simulation parameters.
   - **b)** Water flow parameters.
   - **c)** Atmospheric parameters.
   - **d)** Kriging parameters.
   - **e)** Snow parameters.
   - **f)** Initial soil moisture parameters.

7.1.1 Input output file names

The input output file names have to be written in the same order used by the program. More detailed information on each file is reported in the following sections.

7.1.2 Parameters

We report here a brief description of all parameters, with the name of the parameter in the source code and a indicative value.

7.1.3 Control simulation parameters

DT3 50 - 300 [s] Simulations time step. This parameter controls the programs computational velocity. Too much large time step can cause numerical instability in the ground heat flux calculation. This happens often due a large variation of the atmospheric forcing.

d_inizio 1 - 365 : the day of begin simulation. It is referred to the beginning of the meteorological input data set, and not to the years date.

TH 1 - 365 : the number of simulations days.

state 0 - 1 : 0 if you do not know the initial soil moisture state, 1 otherwise (you need also the initial soil moisture input file)

state1 0 - 1 : 0 if you do not have measured shortwave radiation in the meteorological input data set, 1 otherwise (see 3.3 for the calculation of shortwave radiation).

state2 0 - 1 : 0 if you do not have measured diffuse shortwave radiation, 1 otherwise (see 3.3 for the calculation of diffuse radiation).

state3 0 - 1 : 0 if you do not have a file with cloud cover observations (based for example on SYNOP observations), 1 otherwise.

dmip_flag 0 -1 : 1 if you have DMIP input meteorological data, 0 otherwise.

- The standard format is: 1) MM; 2) DD; 3) HH; 4) YYYY; 5) V [m/s]; 6) Rh [%]; 7) P [hPa] 8) Ta [C]; 9) Rad sw [W/m^2]; 10) Rad diff [W/m^2]; 11) Rad net [W/m^2];
- The DMIP format is: 1) MM; 2) DD; 3) HH; 4) YYYY; 5) V [m/s]; 6) Pv [hPa]; 7) P [hPa]; 8) Ta [C]; 9) Rad sw [W/m^2]; 10) Rad lw [W/m^2]; 11) ρ air [kg/m^3];

state4 0 - 1 : 1 if you want display output for a specified pixel (the program writes the file *output5.txt*, which contains all the results in a particular point), 0 otherwise. With this option, the program writes several quantities for a selected control pixel (further details below).

r_contr 1 - rows number : the row number of the control pixel (if state4=1).

c_contr 1 - columns number : the column number of control pixel (if state4=1). It is important that the control pixel is inside the boundaries of the basin.

delta_tempo_output 1 - hours simulation : the time interval [h] when you want that the program writes output matrices. Each delta_tempo_output hours, the program writes several output matrices with different quantities (further details below). For example, if you want daily averaged soil moisture maps of the basin, delta_tempo_output have to be set to 24 hours.

delta_tempo_stazione 1 - hours simulation : the times interval when you want output for a specified pixel [h], also the time step of the file *output5.txt*.

err_massa 0.001 - 0.05 : the maximum percent error allowed in the mass conservation. During the simulation, the program may cumulate a little numerical error in mass conservation. If the error increases quickly, often it is caused by inconsistencies in the input files.

n_layer 3 - 6 : the number of soil layer used in the soil heat flux calculation. Increasing the number of layer increases the numerical accuracy and the computational time. Too thin layers can also cause numerical instability.

err_l 0.00001 - 0.01 : the error for the Crank Nicolson method, used in the soil heat flux calculation. Usually the convergence is easy to obtain.

l_max 3 - 20 : the maximum number of iteration for the Crank Nicolson method. Usually the convergence is obtained with a few iterations.

7.1.4 Water flow parameters

u 0.5 - 5 [m/s]: the mean velocity in channels.

D 10 - 1000 [m^2/s]: the hydrodynamical dispersion in channels.

cost_sub 0.000005 - 0.0005 [m/s]: the mean velocity of the subsurface flow.

dev_sub 0.00003 - 0.0003 [m/s]: the standard deviation of subsurface velocity. It is assumed to be spatially lognormal distributed, with a known standard deviation.

cost_sup 0.1 - 1 [m/s]: the mean velocity of the surface flow.

dev_sup 0.001 - 0.1 [m/s]: the standard deviation of surface velocity. It is assumed to be spatially lognormal distributed, with a known standard deviation.

cost_inf 0.000035 - 0.0005 [m/s]: the infiltration velocity

f_perm 0.01 - 10 [m^{-1}]: the decay factor of the hydraulic conductivity with the depth. The hydraulic conductivity it is assumed to decay exponentially with depth, following the equation (Franchini, 1996):

$$K_s = \frac{K_{so}}{f\_perm} \frac{\exp(-f\_perm \cdot h_w) - \exp(-f\_perm \cdot h_s)}{h_s - h_w} \tag{7.1}$$

where K_s is the mean equivalent hydraulic conductivity, K_{so} is the surface hydraulic conductivity, h_w is the water table depth, and h_s is the soil depth.

Values of f_perm below 0.01 approximate a situation with no permeability decay.

h_crit 0.1 - 3 [m]: the soil depth in convergent zones (see par. 3.5).

threshold 0.2 - 10 [m]: the threshold stress value. If the local stress (following the equation 3.64) is bigger than this threshold value, the pixel is defined as a channel (see par. 3.6).

wt_max 1 - 10 [mm]: the maximal vegetation interception.

7.1.5 Atmospheric parameters

10, h0_z0 [ ]: the rate h_0/z_0 (see eq. 3.37).

d0_h0 0 - 10 [ ]: the rate d_0/h_0 (see eq. 3.37).

z0_zt 1 - 10 [ ]: the rate z_0/z_t (see eq. 3.37).

c_rad 0.2 [ ]: the coefficient of atmospheric attenuation. It is the product of scattering factor and turbidity factor ($n \cdot a1$) in equation 3.18.

c1_nubi 0.6 [ ]: the first coefficient of cloud attenuation: c_1 in equation 3.17.

c2_nubi 2.5 [ ]: the second coefficient of cloud attenuation: c_2 in equation 3.17.

intervallo_escursione 7 [days]: the number of day of mobil mean for calculating the annual excursion of temperature. This parameter and the following are used for the lower boundary condition in ground heat flux calculation.

sfasamento 109 [days]: the day in which the temperature is the mean temperature. It is the phase displacement $\delta_{gg} = 109\ gg$ in equation 3.62.

7.1.6 Kriging parameters

varianza 0.5 - 2 [$(mm/dt)^2$] spatial variance of precipitation (σ^2 in equation 3.1).

scala_integr 5000 - 20000 [m] integral scale of precipitation (L in equation 3.1).

7.1.7 Snow parameters

Snow parameters follow the snow melt model of Tarboton (1995). Up to now, this part is not yet finished.

t_rain 3 [C]: temperature above which all precipitation is rain.

t_snow -1 [C]: temperature below which all precipitation is snow.

aep 0.1 [m]: albedo extinction parameter.

avo 0.85 [ ]: new snow visible band reflectance.

airo 0.65 [ ]: new near infrared band reflectance.

lc 0.05 [ ]: liquid holding capacity of snow.

snow_inf 0.00555 [m/s]: snow saturated hydraulic conductivity.

7.1.8 Initial soil moisture parameters

Those parameters are used only if do not exist a initial soil moisture input file (state=0) The initial soil moisture can be given with different values, depending from the topographic index (Eq. 7.2) .

UR_1 0 - 1 [ ]: initial saturation in zone 1: cells where the topographic index has a high value.

UR_2 0 - 1 [ ]: initial saturation in zone 2: cells where the topographic index has a mean value.

UR_3 0 - 1 [ ]: initial saturation in zone 3: cells where the topographic index has a low value.

7.1.9 Example of the file *geo_top.inpts*

```
/*************************************************************
FILE GEO_TOP.INPTS WITH I/0 FILES NAMES
AND SIMULATION PARAMETERS
*************************************************************

*************************************************************
1) INPUT OUTPUT FILES:
*************************************************************

input1, input2, input3, input4, input6, input7, input8, input9,
input10, input11, output1, output2, output3, output4, output5,
output6, output7 */

index{2}

1:string array IO files
{ washita.dem.txt, washita.sky.txt, washita.rain.txt,
```

```
washita.meteo.txt, wahita.par.txt, washita.cover.txt,
washita.cloud.txt, washita.albedo.txt, washita.class.txt,
washita.snow.txt, output1.txt, output2.txt, output3.txt,
output4.txt, output5.txt, output6.txt, output7.txt }

/*********************************************************
2) PARAMETERS
*********************************************************

DT3, d_inizio, TH, state, state1, state2, state3, dmip_flag,
state4, r_contr, c_contr, delta_tempo_output,
delta_tempo_stazione, err_massa, n_layer, err_l, l_max, u,
D, Cost_sub, Dev_sub, Cost_sup, Dev_sup, Cost_inf, f_perm,
h_crit, threshold, Wt_max, h0_z0, d0_h0, z0_zt, c_rad,
c1_nubi, c2_nubi, intervallo_escursione, sfasamento,
varianza, scala_integr, t_rain, t_snow, aep, avo,  airo, lc,
snow_inf, UR_1, UR_2, UR_3 */

2: double array parameters
{ 100, 1, 25, 0, 1, 0, 1, 0, 1, 25, 155, 24, 1, 0.01, 3,
0.001, 5, 2.5, 1000, 2E-3, 0.000003, 0.30, 0.001, 3E-6, 0.01,
0.16, 0.15, 4, 10, 0, 1, 0.2, 0.6, 2.5, 7, 90, 1, 10000, 3,
-1, 0.1, 0.85, 0.65, 0.05, 0.00555, 0.4, 0.4, 0.4 }
```

7.2 Input 1: File elevation

Il *File elevation* is a matrix, where each element is the elevation of the terrain on the see surface.

7.2.1 Example of *File elevation*

```
/** Little washita DEM */

index {3}
1: float array dem header {200,200,562000,3847000}
2: float array novalue {-1,-9}
3: float matrix DEM {140,220}

... matrix elements ...
```

7.3 File Sky

The *File Sky* contains the sky view factor of each point of the basin. This file is calculated separately with the program *Sky.c*(Verardo, 1998). The program is explained in B. The sky view factor is the angular fraction of sky visible from a point. Without obstructions, the factor is 1 and in a mountain environment the factor can be less than 0.6 and can be important take it in account for evaluate the diffuse solar radiation.

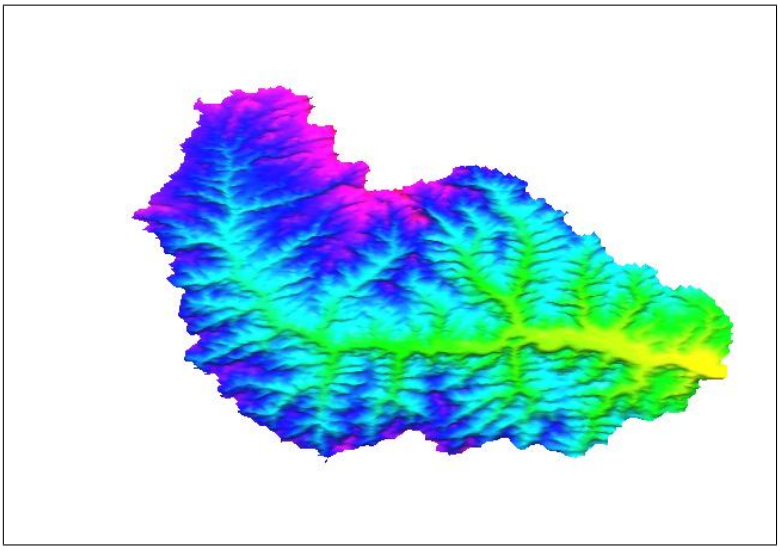

Figure 7.1: *Example of elevation map. Here is presented the Little Washita basin (OK, USA). Higher elevations are red, lower yellow.*

7.3.1 Example of *File Sky*

```
/** This_is_a_turtle_file created on Aug  7 2001
at 13:00:45 by SkyViewFactor
inputs processed :
C:\075\DATA\geotop\SGP97\SkyViewFactor */

index{3}
1: float array dem header
{200.000000,200.000000,562000.000000,3847000.000000}
2: float array novalues {-1.000000,-9.000000}
3: float matrix sky {140,220}
... matrix elements ...
```

7.4 File Rain

The *File Rain* contains the hourly precipitation data $[mm]$ and the coordinates of all raingages or of the center of radar cells. The rain data have the same temporal duration as the meteorological data, and the coordinates are in the same units as the DEM coordinates.

The file is divided in two blocks:

1. Matrix with precipitation data.

2. Matrix with coordinates (Longitude $[m]$, Latitude $[m]$).

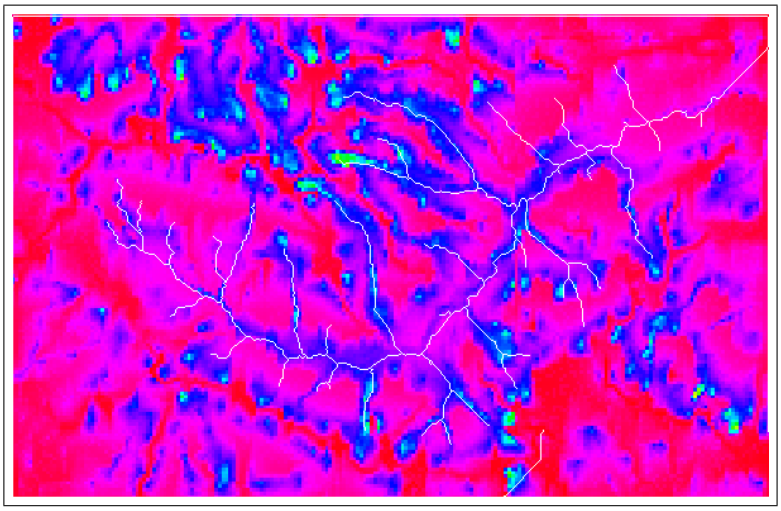

Figure 7.2: *Example of sky view factor map. Here is presented the Little Washita basin (OK, USA). Values change from 0.9 (green) to 1 (red).*

7.4.1 Example of *File Rain*

```
/** Matrix with precipitation data -
    Oklahoma Mesonet raingauges -
    year 1997 data each hour [mm/h] -
    stations A110 A111 A121 A122 */

index {2}
1: float matrix rain {2304,4}
0     0    0.4  0
0.2   0    0.5  0
1.5   2.0  0    0
...   ...  ...  ...

2: double matrix coordinates {4,2}
590728.5    3874885.3
595635.5    3875110.7
600568.7    3868818.5
595594.3    3870335.5
```

7.5 File Meteorological Data

The required *meteorological data* are the following:

- MM = month;
- DD = day;
- HH = hour;

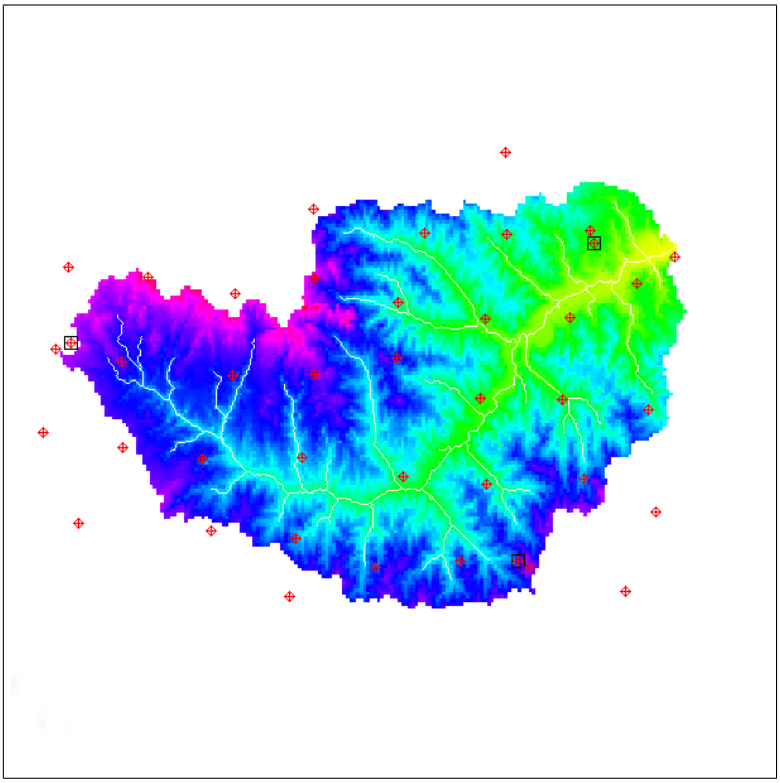

Figure 7.3: *Example of elevation map. Here is presented the Little Washita basin (OK, USA). The map resolution is 200 m. Red rombes are raingages, black squares are complete meteorological stations.*

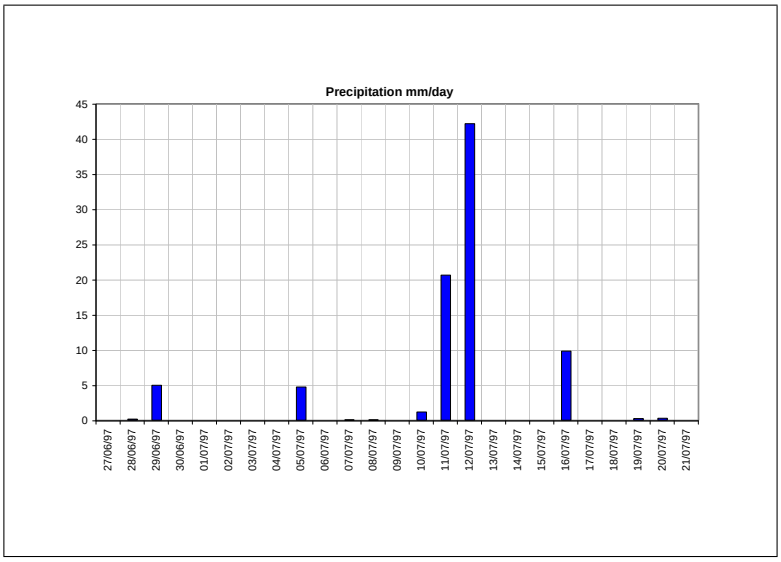

Figure 7.4: *Example precipitation time series. Here is presented the daily averaged precipitation on the the Little Washita basin (OK, USA).*

- $YYYY$ = year (the date is not read by the program, it serves only for reference);
- V = wind speed $[m/s]$;
- R_h = relative humidity [%];
- P_a = air pressure $[hPa]$;
- T_a = air temperature $[C]$;
- $R\downarrow_{SW}$ = $[W/m^2]$(optional);
- $R\downarrow_{SWdiff}$ = diffuse shortwave radiation $[W/m^2]$ (optional);
- R_n = net radiation $[W/m^2]$ (optional);

If the option *"DMIP format"* is chosen, instead of relative humidity R_h there is vapor pressure P_v $[hPa]$, instead of diffuse shortwave radiation $R\downarrow_{SWdiff}$ there is longwave radiation $R\downarrow_{LW}$ and instead net radiation R_n there is air density ρ_a $[kg/m^3]$.

Up to now, the program uses uniform input meteorological data in the basin.

7.5.1 Example of *File Meteo*

```
/** Metereological Forcing data from 01/01/1997 to 31/12/1997
Little Washita mesonet station ACME */

index{4}

/** Latitude, longitude (rad), elevation (m),
sky view factor of meteorological station */
```

```
1:float matrix station {1,4}
0.608218 -1.71057 398.3 0.98

/** Wind speed measurement height (on the ground) [m],
humidity and temperature measurement height [m] */
2:float matrix sensors {1,2}
10  1.5

/** Julian day and hour (UTC) of begin data set,
time step [h] */
3:float matrix times {1,3}
178 00  1

/** MM GG HH AAAA V(m/s) Rh% Pa(hPa) Ta(C) Rad_sw(W/mq)
Rad_diff(W/mq) Rad_net(W/mq)*/

4: float matrix data {2304,11}
... meteo data ...
```

7.6 File Soil

The *File soil* contains several parameters, which are constant for the whole basin. They are indicated below, with an indicative value, in the order of programs reading.

7.6.1 Soil production model parameters

m = **5.0 [**m^{-1}]: the inverse of the soil production for unit time;

P_0 = **0.00019 [m**]: the soil production at the initial instant;

prs = **1.7 [**]: the rate between the rock's porosity ρ_r and the soil's porosity ρ_s.

k = **0.005 [**m^2]: the soil's production diffusivity.

7.6.2 Soil's proprieties

ρ_s = **1200 [**kg/m^3]: soils density;

c_s = **800 [**$J/(kgK)$]: soils specific heat;

k_s = $0.2 \cdot 10^{-6}$ **[**m^2/s : soils thermic diffusivity;

ϵ_s = **0.96 [**]: soils emissivity.

If experimental data are not available, literature values of those parameters can be found in Clapp and Hornberger, (1978).

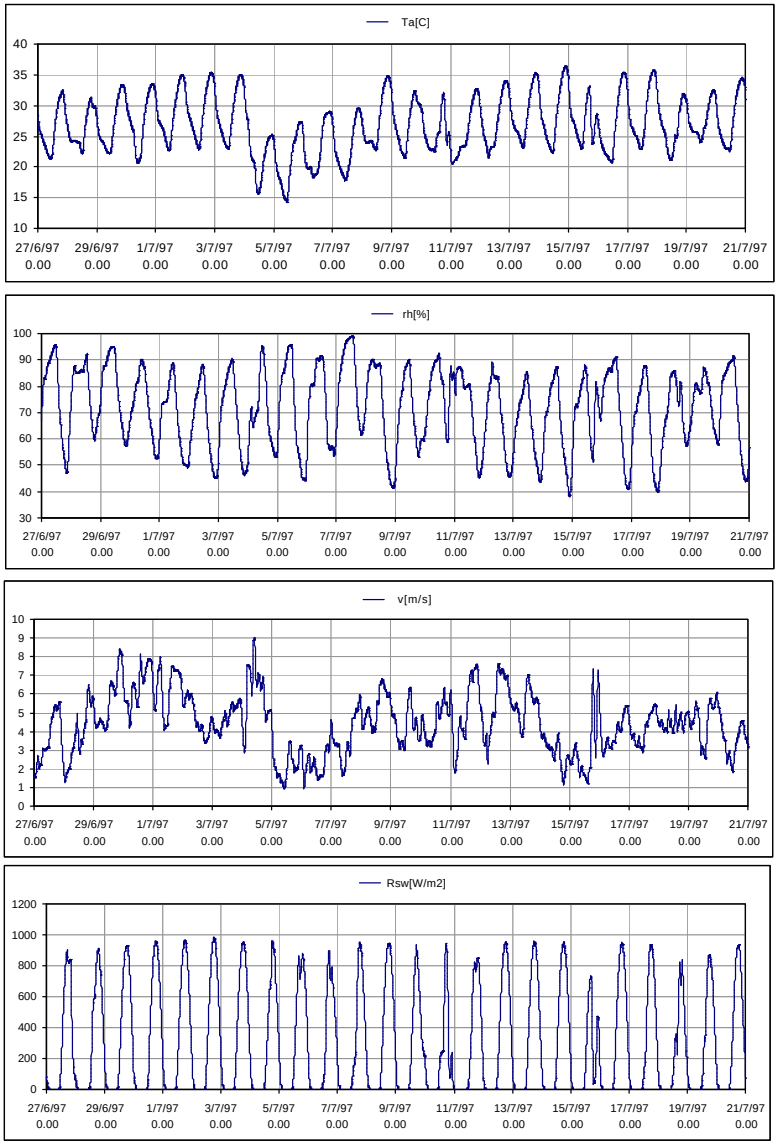

Figure 7.5: *Example meteorological input data time series (Little Washita basin OK, USA).*

7.6.3 Snows proprieties

ρ_i = **917 [**kg/m^3]: ices density;

ρ_i = **450 [**kg/m^3]: snows density;

ρ_i = **2090 [**$J/(kgK)$: ices specific heat;

ρ_i = $5.55 \cdot 10^{-6}$ **[**m^2/s]: snows thermic diffusivity;

ϵ_{snow} = **0.95 [**]: new snows emissivity.

7.6.4 Example of *File soil*

```
/** Matrix soil parameters {13,1}
1) Soil production model parameters:
m [1/m], P [m], prs [], k [m^2]
2) Soils proprieties:
rho_s [kg/mc^3], c_s [J/(kg K)], k_s [m^2/s], epsilon_s []
3) Snows proprieties:
rho_i [kg/m^3], rho_snow [kg/m^3], c_i [J/(kg K)],
k_snow [m^2/s], epsilon_snow [] */

index{1}
1:double matrix parameters {13,1}
0.00019 5.0 1.7 0.005 1200 800 0.2E-6 0.96 917 450 2090
5.55E-6 0.95
```

7.7 File Land Cover Classification

In this file is specified the land cover classification used by the program. It is possible to specify several different types. For each type is specified the roughness (canopy or buildings mean height) and the canopy fraction (the fraction of bare ground covered by leaves). If the surface is a water body (water body is always the number 4), changes also the albedo and the heat fluxes parameterization.

7.7.1 Example of *File Land Cover Classification*

```
/** Land cover classification:
row1: Classes: 0=other 1=wood 2=grass 3=urban 4=water
row2: Canopy height hc [m]:
row3: Canopy fraction fc */

index{1}
1: float matrix classification {3,5}
... data ...
```

7.8 File Land Cover Map

In this file is written the land cover matrix, according tho the codes specified in the previous file.

7.8.1 Example of *File Land Cover map*

```
/** Land Cover: 0 other 1=trees 2=grass 3=urban 4=water */

index {3}
1: float array dem header {200,200,562000,3847000}
2: float array novalue {-1,-9}
3: short matrix DEM {140,220}
... data ...
```

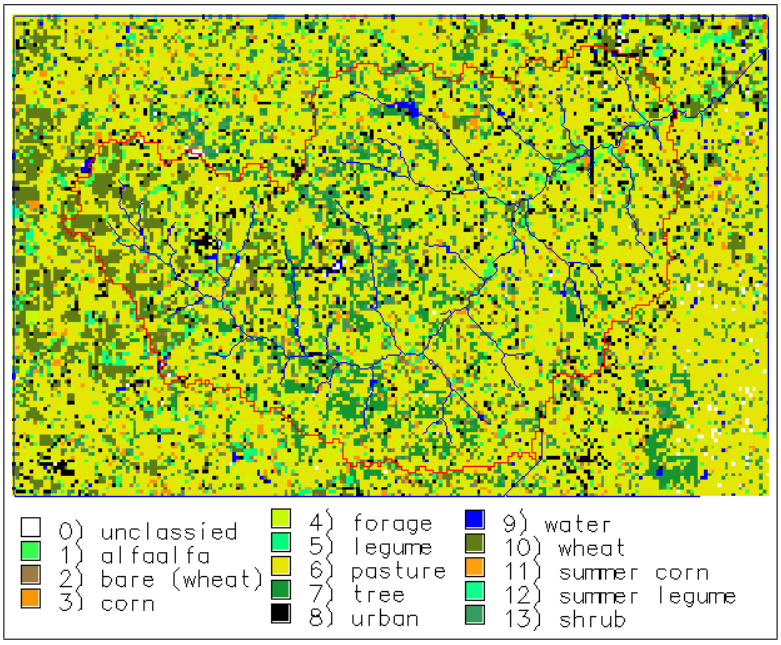

Figure 7.6: *Example land cover map. Here is presented the Little Washita basin (OK, USA).*

7.9 File Albedo Map

Il *File Albedo Map* contains the matrix with the bare ground albedo (range 0 - 10) for the basin.

7.9.1 Example of *File Albedo Map*

```
/** Little Washita bare soil albedo DEM */
```

```
index {3}
1: float array dem header {200,200,562000,3847000}
2: float array novalue {-1,-9}
3: float matrix albedo {140,220}
... data ...
```

7.10 File Cloud Cover

The *File Data Cloud Cover* is a matrix with two columns with values of:

N_{tot}**:** total cloud cover in octaves (0=clear, 8=covered, 9=sky no visible or clouds extension not valuable;

NH**:** sky fraction covered by low clouds (CL) or, if there are not those, sky fraction covered by mean clouds (CM).

This file is optional. If it not exist, the parameter $state3$ have to be set to 0 and clear sky is assumed.

7.10.1 Example of *File Data Cloud Cover*

```
/** Synop Data Cloud Cover L.Washita 1997

index{3}
/** array times: julian day of begin data; time step [h] */
1: float array times {1,24}
2: float array novalue {-99}
/** matrix cloud: NTOT(ott)   NH(ott) */
3: float matrix cloud {365,2}
0  0
1  0
2  1
8  8
...
```

7.11 File Snow Cover Map

The *File Snow Cover Map* contains the matrix with the initial snow cover water equivalent [mm] for the whole basin.

7.11.1 Example of *File Snow Cover Map*

```
/** Little Washita initial snow water equivalent DEM */

index {3}
1: float array dem header {200,200,562000,3847000}
2: float array novalue {-1,-9}
```

```
 3: float matrix snow {140,220}
... data ...
```

7.12 File Initial Soil Moisture

This file is needed if the option $state1$ is set to 1. It is build by three matrices with the initial water volume in each pixel [m^3] for (1) Vol_{sur} the *surface layer* , (2) Vol_{uns} the *unsatured upper layer* and (3) Vol_{sat} the *lower satured layer*.

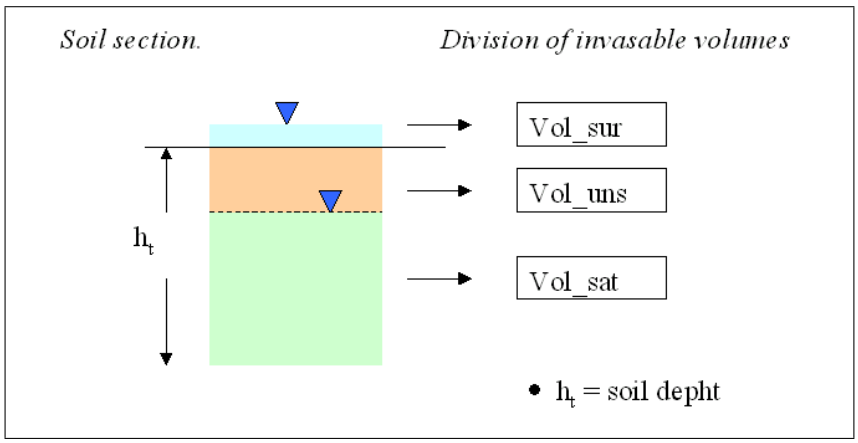

Figure 7.7: *Soils water content layers used by the program: (1) Vol_{sur} water content in the* surface layer *, (2) Vol_{uns} water content in the* unsatured upper layer *and (3) Vol_{sat} water content in the* lower satured layer.

The initial water content can be assigned a priori, or using a the output of a pre conditioning simulation. If this information is unavailable, the initial value is assigned following the *topographic index* (Beven e Kirkby 1979, Franchini et al. 1996, Pegoretti 1999). The topographic index is defined as:

$$Top_{ind} = \log\left(\frac{A_c}{i}\right) - \mu \tag{7.2}$$

where A_c is the cumulated up slope area, i is the local slope, μ is the mean topographic index for the whole basin. A point with less slope and more up slope area have a bigger saturations probability.

All points are divided in three classes of topographic index, and the user can set a different value of initial saturation for each class, playing on the parameters *UR_1*, *UR_2* and *UR_3*.

7.12.1 Example of *File Initial Soil Moisture*

```
/** Water volume in each pixel [mc]: vol_sur (surface),
vol_uns (upper unsatured layer), vol_sat (lower satured layer) */

index{5}
```

```
1:float array pixels size
{200.000000,200.000000,562000.000000,3847000.000000}
2:float array novalues {-1.000000,-9.000000}

3:double matrix vol_sur {140,220}
... data ...

4:double matrix vol_sat {140,220}
... data ...

5:double matrix vol_ins {140,220}
... data ...
```

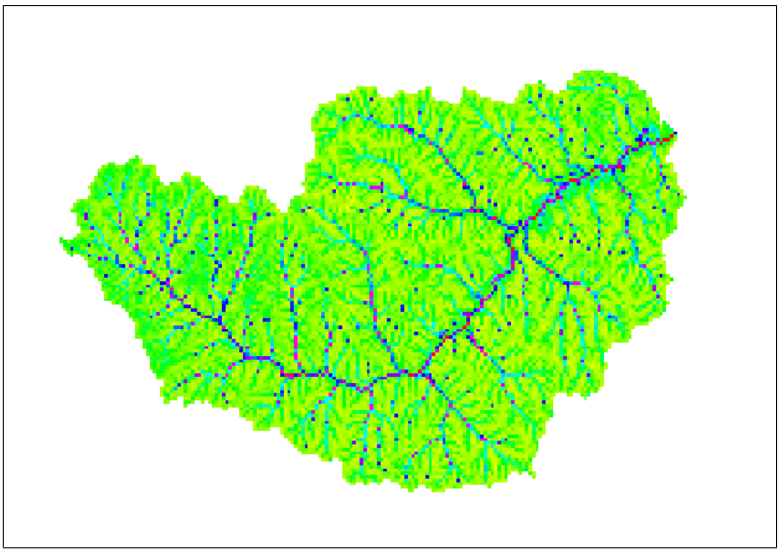

Figure 7.8: *Example of topographic index map for the (Little Washita basin, OK, USA). If the initial soil moisture is not known, it can be assigned according the topographic index.*

Chapter 8

Output Data Files

The program gives several output files, with different spatial and temporal resolution:

- Time series for a specific pixel;
- Time series of mean values on the whole catchment;
- Matrices with values for all pixels, given as mean on a given times.
- Matrices with values for all pixels at the end of the simulation.

8.1 OUTPUT1.TXT

This file contains:

1. The total water volumes flowed during the simulation [m^3]: initial water volume, total discharge, final water volume, total precipitation, total evapotranspiration.
2. The discharge at the outlet, given each **DT3** (defined in paragraph 7.1) time step: time [h], subsurface flow [m^3/s], surface flow [m^3/s], total flow [m^3/s] (surface and subsurface).

8.1.1 Example of *Output1*

```
index{2}
1:float array state of basin
/** Total water volumes flowed during the simulation [$m^3$]:
Input: initial water volume;
Output: total discharge;
Dentro: final water volume;
Pio_Tot: total precipitation;
Evapo_Tot: total evapotranspiration. */
43364065.340 7164757.566 26611523.382
49057619.493 58615469.138
```

```
2:float matrix responce{7201,4}
/** Time interval is DT
t[h]     Q_subsur[mc/s] Q_sur[mc/s] Q_tot[mc/s] */
0.000000 0.000000       0.000000    0.000000
0.083333 0.000670       0.000210    0.000880
...      ...            ...         ...
```

8.2 OUTPUT2.TXT

If the outlet section of the basin is a lake, this file contains the water input in the lake, without the river network contribute (reported in *OUTPUT1.txt*). The files contains also, the water flow coming from the hillslopes, and the water precipitating directly on the lake. The file has a matrix with the water flow [m^3/s], given each time step (**DT3**, defined in paragraph 7.1).

8.2.1 Example of *Output2*

```
/** Water flow [mc/s] coming in to the lake.
Time interval is DT3  */

index{1} 1:float matrix water_into_lake{7201,1}
0.000000
0.200000
...
```

8.3 OUTPUT3.TXT

This file contains the final water content of the basin. It have the same structure as the *initial soil moisture file*, explained in the paragraph 7.12. It contains the matrices with the water content [m^3], for (1) Vol_{sur} the *surface layer* , (2) Vol_{uns} the *unsatured upper layer* and (3) Vol_{sat} the *lower satured layer*. This file can be used, without changes, as input (initial condition) for a subsequent simulation.

8.4 OUTPUT4.TXT

This file contains values averaged on the basin of the terms of the water and energy balance. If a lake is present, there is also reported the averages for the lake surface only. Time interval is (**DT3** (defined in paragraph 7.1). The columns are:

1. **t** time from beginning simulation [h] ;
2. **Prec** total precipitation [m^3/s];
3. **Evapo** total evapotranspiration [m^3/s];
4. **Rn** net radiation [W/m^2];

5. **G** soil heat flux [W/m^2];
6. **H** sensible heat flux [W/m^2];
7. **Et** latent heat flux [W/m^2];
8. **E** energy storage [W/m^2];
9. **Prec_lake** total precipitation in to the lake [m^3/s];
10. **Evapo_lake** total evaporation in to the lake [m^3/s];
11. **Rn_lake** net radiation in to the lake [W/m^2];
12. **G_lake** energy flux in to the lake [W/m^2];
13. **H_lake** sensible heat flux in to the lake [W/m^2];
14. **Et_lake** latent heat flux in to the lake [W/m^2];
15. **E_lake** energy storage in to the lake [W/m^2];

8.4.1 Example of *Output4*

```
index{1}
1:float matrix phis_matrix{7201,15}
/** Time interval is DT3:
t[h] Prec[mc/s] Evapo[mc/s] Rn[W/mq] G[W/mq] H[W/mq] Et[W/mq]
E[W/mq] Prec_lago[mc/s] Evapo_lago[mc/s] Rn_lago[W/mq]
G_lago[W/mq] H_lago[W/mq] Et_lago[W/mq] E_lago[W/mq] */
...
data
...
```

8.5 OUTPUT5.TXT

If the flag **state4** is activated (see paragraph 7.1), the program writes the file *output5.txt*, which contains much information on a particular point. With this option, the program writes several quantities for a control pixel, selected by the flags **r_contr** and **c_contr**. The time step of the results can be specified by the flag **delta_tempo_stazione**. In the file are also reported several information on the simulation (see example below).

The quantities written for the control pixel are the following:

1. t time from simulations begin [s];
2. dd years julian day;
3. hh days hour;
4. v input wind speed [m/s];
5. Wa measured relative humidity [ ];

6. P measured atmospheric pressure [hPa];
7. T_a measured air temperature [^oC];
8. $R\downarrow_{SW}$ shortwave radiation [W/m^2];
9. $albedo$ ground albedo [ ];
10. T_{sn} lowest soil layer temperature [^oC];
11. $Prec$ precipitation [mm];
12. R_n net radiation [W/m^2];
13. G soil heat flux [W/m^2];
14. H sensible heat flux [W/m^2];
15. ET latent heat flux [W/m^2];
16. $\Delta E/\Delta t$ energy storage in the canopy layer [W/m^2];
17. C_{Dn} neutral drag coefficient [ ];
18. C_{Hn} neutral heat transfer bulk coefficient [ ];
19. $F_M = C_D/C_{Dn}$
20. $F_H = C_H/C_{Hn}$
21. Ri_B bulk Richardsons number;
22. Vol_{sur} water volume in the surface layer [mm];
23. Vol_{uns} water volume in the unsatured upper layer [mm];
24. Vol_{sat} water volume in the lower satured layer [mm];
25. W_t canopy intercepted water [mm];
26. $Prec_{net}$ net precipitation [mm];
27. E_{VC} wet canopy evaporation [mm];
28. E_{TC} dry canopy transpiration [mm];
29. E_G bare soil evaporation [mm];
30. ET total evapotranspiration [mm];
31. ET_{PM} latent heat flux, calculated using the Penman-Monteith equation [W/m^2];
32. H_{PM} sensible heat flux, calculated using the Penman-Monteith equation [W/m^2];
33. r_c evaporations canopy resistance [s/m];
34. ρ_s soil density
35. c_s soil specific heat [J/kg];
36. k_s soil thermic diffusivity [m^2/s];
37. sat soil saturation rate [ ];
38. $T_s ... T_{n-layer}$ soils temperature, for all soil layers [^oC].

8.5.1 Example of *Output5*

```
/** A few outputs for the pixel row 25, col 155:*/
index{8}

/** Pixel position: dx, dy, xo, yo */
1:float array pixels size
{200.000000,200.000000,562000.000000,3847000.000000}

/** DTM: matrix 220 rows X 140 cols */
/** pixels number =30800,
    valid pixels  =16223,
    pixel novalue =14577 */

/** Simulations control parameters, as in the input
file geotop.inpts */
2:float array parameters
{300.000000,1.000000,25.000000,0.000000,1.000000,0.000000,1.000000,
0.000000,1.000000,25.000000,155.000000,24.000000,1.000000,0.010000,
3.000000,0.001000,5.000000,3.000000,10.000000,0.001000,0.000003,
0.600000,0.001000,0.000002,0.010000,2.500000,0.150000,4.000000,
10.000000,0.000000,1.000000,0.200000,0.600000,2.500000,7.000000,
90.000000,1.000000,10000.000000,3.000000,-1.000000,0.100000,
0.850000,0.650000,0.050000,0.005550}

/** Soils parameters, as in the input file soil: P, m, prs, k,
rho_s, c_s, k_s, epsilon_s */
3:double matrix soil_parameters {8,1}
0.000190 5.000000 1.700000 0.005000 1200.000000 800.000000 0.000000
0.960000 917.000000 450.000000 2090.000000 0.000006 0.990000

/** Meteo station latitude [rad], longitude,
elevation [m], sky view factor */
4:float matrix station {1,4}
0.608218 -1.710570    398.299988    0.980000

/** Wind measurement height [m above the ground],
temperature and relative humidity height [m above the ground]*/
5:float matrix sensors {1,2}
10.000000    1.500000

/** Aerodynamic roughness length [m], displacement height [m],
bulk roughness length [m] */
6:float matrix roughness {1,3}
0.050000, 0.000000, 0.050000

/** Other proprieties of the control pixel:
slope = 1.955598 [deg]
aspect = 29.391445 [gradi, 0=N, orario]
void volume = 41176.468750 [mc]
```

```
fraction of canopy cover= 0.000000 */

/** Soil layers thickness (for heat calculation)[m]*/
7:double array thickness
{0.099757,0.136507,0.770956}

/* Data for the control pixel, given each time step
(defined by delta_tempo_stazione),
first line after 0.5 time step,
julian day from the years begin */

8:float matrix point data {0,39}
time[s], day, hour, v[m/s], Wa[0-1], P[hPa], ta[C],
R_sw[W/m^2], albedo[0-1], Ts_n_layer[C], Prec[mm], Rn[W/m^2],
G[W/m^2], H[W/m^2], ET[W/m^2], E_imm[W/m^2], CDn[], CHn[], FM[],
FH[], Rib[], Vol_sur[m^3], Vol_uns[m^3], Vol_sat[m^3],
W_t[m^3], Prec_net[m^3/DT], Vol-Evc[m^3/DT], Vol-Etc[m^3/DT],
Vol-Eg[m^3/DT], Vol-ET[m^3/DT], Et_PM[W/m^2], H_PM[W/m^2],
r_c[s/m], ro_s[kg/m^2], c_s[J/(kg/K)], k_s[m^2/s], sat[0-1],
T1[C], ..., Tn_layer[C] */
... data ...
```

8.6 OUTPUT6.TXT

If the flag **state4** is activated (see paragraph 7.1), the program writes the file *output6.txt*. With this option, the program writes the mean values for the whole basin (differently from *output5.txt*) of several quantities, related to the mass and energy balance. The time step of the results can be specified by the flag **delta_tempo_output** and it is the same than the time step of the intermediate output files (see paragraph 8.8.2).

The quantities written for the control pixel are the following:

1. t time from simulations begin [s];
2. dd years julian day;
3. hh days hour;
4. $Input$ total initial water volume in the basin at the beginning of simulation [m^3];
5. $Dentro$ total water volume in to the basin at the current time [m^3];
6. $Output$ total discharge from the basin from the beginning of simulation to the current time [m^3];
7. Pio_Tot total precipitation in the basin from the beginning of simulation [m^3];
8. $Evapo_Tot$ total evapotranspiration in the basin from the beginning of simulation [m^3];
9. $error$ percentage error in the mass balance from the beginning of simulation [%];

10. R_n net radiation [W/m^2];
11. G soil heat flux [W/m^2];
12. H sensible heat flux [W/m^2];
13. ET latent heat flux [W/m^2];
14. $\Delta E/\Delta t$ energy storage in the canopy layer [W/m^2];
15. T_s surface soil temperature [^oC].
16. Vol_{sur} water volume in the surface layer [mm];
17. Vol_{uns} water volume in the unsatured upper layer [mm];
18. Vol_{sat} water volume in the lower satured layer [mm];
19. $Prec_{net}$ net precipitation [mm];
20. W_t canopy intercepted water [mm];
21. ET_{PM} latent heat flux, calculated using the Penman-Monteith equation [W/m^2];
22. H_{PM} sensible heat flux, calculated using the Penman-Monteith equation [W/m^2].

8.6.1 Example of *Output6*

```
/* Mean vales for the whole basin,
   given each delta_tempo_output   */

/**time[s], dd, hh, Input[m^3], Dentro[m^3], Output[m^3],
Pio_Tot[m^3], Evapo_Tot[m^3], error_perc[], Rn[W/m^2],
G[W/m^2], H[W/m^2], ET[W/m^2], E[W/m^2], Ts[C],
vol_surf[mm], vol_ins[mm], vol_sat[mm], prec_net[mm/DT],
Wt[mm], ET_PM[W/m^2], H_PM[W/m^2]*/
... data ...
```

8.7 OUTPUT7.TXT

This is a control file, with possible errors, happened during the program run.

8.8 Debug output files

The program gives also a number of output files, at the beginning of the simulations (preliminary geomorphological analysis matrices) and during the simulation (temporary state of the basin).

8.8.1 Initial control matrices

At the beginning of simulation, the program writes several matrices, with intermediate results. Those data are useful to control the simulation and are written in the files:

Prova.albedo.txt : File with the *albedo* matrix (see par. 7.9).

Prova.amp_mod.txt : File with the *distance of each point from the basins outlet*: it contains the distance (positive values) of a channel pixel from the outlet and the distance (positive values) of a hillside pixel from the nearest channel pixel (see par. 4).

Prova.area.txt : File with the *area* of each cell (considering the real slope).

Prova.azimuth.txt : File with the *aspect* matrix (radians, 0 N, hourly direction) (see par. 4).

Prova.ca.txt : File with the *up slope contributing area* (in pixels) (see par. 4).

Prova.canopy_cover.txt : File with the *canopy cover fraction* (0 - 1), as specified in the input files *Land Cover Classification* and *Land Cover Map* (see par. 7.7).

Prova.channelsixeldistance.txt : File with the *distance of each channel pixel from the outlet* (in pixels, 0 hillslope, 1 outside the basin).

Prova.curv.txt : File with the *laplacian* ($\nabla^2 z$) of the topography (see par. 4).

Prova.curv1.txt : File with conventional values of the *laplacian*: 1 for convergent zones ($\nabla^2 z > 0$), 0 for divergent zones ($\nabla^2 z > 0$).

Prova.drainage_direction.txt : File with *gradients*, computed as in par. 4.

Prova.m.txt : File with *drainage directions*, computed as in par. 4.

Prova.m_mod.txt : File with the river network (code 10), superimposed on the drainage directions.

Prova.p_mod.txt : File with the *precipitation*, given for each measurement station and each computational time step. The first column is the time from the begin of simulation in seconds.

Prova.pond_volume.txt : File with water volume in each pixel [m^3] for the *surface layer* (Vol_{sur}), as explained in the paragraph 7.12.

Prova.slopes.txt : File with the *slope* matrix (radians,) (see par. 4).

Prova.soil_moisture.txt : File with water volume in each pixel [m^3] for the *lower satured layer* (Vol_{sat}), as explained in the paragraph 7.12.

Prova.spessori.txt : File with the *thickness* of the layers [m], used in the calculation of the soil heat flow (see par. 3.4.5). The user can choose the number of layers in the input routing file *geo_top.inpts*. The integration of the soil heat flux is made on a depth of about 1 m, and the thickness of the layers, to be more accurate on the surface, is increasing exponentially with depth, using the relationship 3.57.

Prova.top_ind.txt : File with the *topographic index*, defined in the equation 7.2.

Prova.vadose.txt : File with water volume in each pixel [m^3] for the *unsatured upper layer* (Vol_{uns}), as explained in the paragraph 7.12.

Prova.vegetazione.txt : File with the canopy height matrix, , as specified in the input files *Land Cover Classification* (see par. 7.7).

Prova.Vol.txt : File with *water storage volume* in the basin: (V_v $[m^3]$) given by the equation 4.1.

Prova.Z0.txt : File with the matrix of *elevations*, cleaned by the eventually present pits. To calculate a coherent drainage network it is necessary to eliminate the pits in the DEM.

8.8.2 Files with intermediate distributed results

If the flag **state4** is activated (see paragraph 7.1), the program writes several output files each **delta_tempo_output** hours. Each file contain a matrix with the results averaged at a given time step.

Each file has a name with a standard codification: *outQQ_NNN.txt*, where the number *NNN* means the time step, and the number *QQ* means the code of the data.

The data reported in the files are the following (the number is the code in the file name):

1. R_n net radiation [W/m^2];
2. G soil heat flux [W/m^2];
3. H sensible heat flux [W/m^2];
4. ET latent heat flux [W/m^2];
5. $\Delta E/\Delta t$ energy storage in the canopy layer [W/m^2];
6. T_s surface soil temperature [^oC].
7. Vol_{sur} water volume in the surface layer [mm];
8. Vol_{uns} water volume in the unsatured upper layer [mm];
9. Vol_{sat} water volume in the lower satured layer [mm];
10. $Prec_{net}$ net precipitation [mm];
11. W_t canopy intercepted water [mm];
12. ET_{PM} latent heat flux, calculated using the Penman-Monteith equation [W/m^2];
13. H_{PM} sensible heat flux, calculated using the Penman-Monteith equation [W/m^2].

For example, if we have a simulation of a week *(TH=7)* and we have daily averages *(delta_tempo_output=24)* the file with the matrix of the mean daily values of latent heat flux *(QQ=04)* for the second day *(NNN=002)* has the name: *out04_002.txt*.

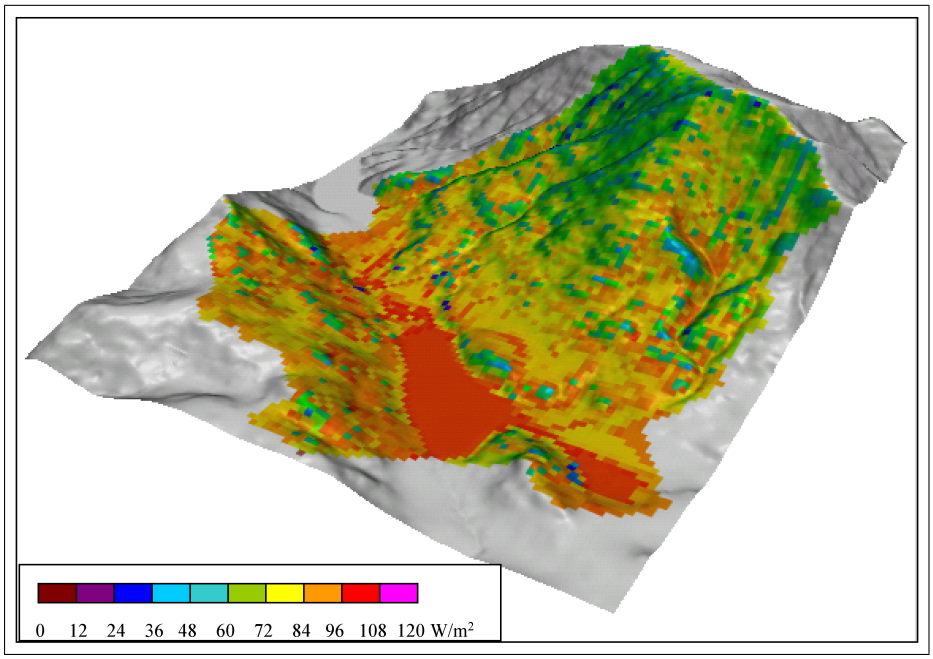

Figure 8.1: *Example evapotranspiration ET for the Serraia basin, Italy. Notice the elevation effect (areas more elevated have less evaporation); the aspect effect (more evaporation in southern slopes, left part of the image); the topographic convergence effect (at the bottom of the valley).*

Appendix A

Compile the Project GEOTOP

The program GEOTOP can be compiled on Windows, Linux and Macintosh. Here are reported all source files required to compile the program. It is also shown an example of Makefile to compile the source code with GCC. The user have only to change the path where the source code is located.

A.1 GEOTOP Source Files

geotop.snow.c

geotop.snow.h

geotop_inputs.snow.c

geotoplib.snow.c

geotoplib.snow.h

hydrology.snow.c

hydrology.snow.h

geomorphology.snow.c

geomorphology.snow.h

networks.c

networks.h

snow.c

snow.h

write_dem.c

write_dem.h

geo_static.c

geo_static.h

A.2 FluidTurtle Source Files

t_io.c

t_io.h

turtle.h

t_list.h

alloc.c

t_alloc.h

error.c

utilities.c

t_utilities.h

tensor3D.h

tensors3D.c

t_statistics.h

linearalgebra.c

linearalgebra.h

random.c

datamanipulation.c

t_datamanipulation.h

t_random.h

A.3 Makefile Example

```
# GEOTOP Makefile

HM              = /mnt/windows/075 LHM     = $(HM)/binaries

LIBPATH1    = $(HM)/LIBRARIES/basics LIBPATH2    =
$(HM)/LIBRARIES/BASICMATHSTAT LIBPATH3    =
$(HM)/LIBRARIES/GEOMORPHOLOGYLIB LIBPATH4    =
$(HM)/LIBRARIES/HYDROLOGYLIB LIBPATH5    =
$(HM)/LIBRARIES/LINEARALGEBRA


NOME        = geotop.exe SCRSPATH1   =
$(HM)/APPLICATIONS/HYDROLOGY/geotop
```

```
BINPATH     = $(LHM)/Bin_linux/geotop BINS        =
$(BINPATH)/$(NOME)

SRCS = $(SCRSPATH1)/geotop.c
    $(SCRSPATH1)/geotop_inputs.snow.c \
    $(SCRSPATH1)/snow.c \
    $(LIBPATH1)/alloc.c
    $(LIBPATH1)/error.c $(LIBPATH1)/list.c
    $(LIBPATH1)/string.c $(LIBPATH1)/t_io.c \
    $(LIBPATH1)/tensors3D.c  $(LIBPATH1)/utilities.c  \
    $(LIBPATH2)/datamanipulation.c
    $(LIBPATH2)/geo_statistic.c
    $(LIBPATH2)/random.c $(LIBPATH2)/statistics.c \
    $(LIBPATH3)/geotoplib.c
    $(LIBPATH3)/geomorphology.c
    $(LIBPATH3)/networks.c \
    $(LIBPATH3)/write_dem.c  \
    $(LIBPATH4)/hydrology.c \
    $(LIBPATH5)/linearalgebra.c

OBJS = $(SCRSPATH1)/geotop.o
    $(SCRSPATH1)/geotop_inputs.o \
    $(SCRSPATH1)/snow.o \
    $(LIBPATH1)/alloc.o
    $(LIBPATH1)/error.o
    $(LIBPATH1)/list.o
    $(LIBPATH1)/string.o
    $(LIBPATH1)/t_io.o \
    $(LIBPATH1)/tensors3D.o
    $(LIBPATH1)/utilities.o \
    $(LIBPATH2)/datamanipulation.o
    $(LIBPATH2)/geo_statistic.o
    $(LIBPATH2)/random.o
    $(LIBPATH2)/statistics.o \
    $(LIBPATH3)/geotoplib.o
    $(LIBPATH3)/geomorphology.o
    $(LIBPATH3)/networks.o \
    $(LIBPATH3)/write_dem.o \
    $(LIBPATH4)/hydrology.o \
    $(LIBPATH5)/linearalgebra.o

HPATH1  = $(LIBPATH1) HPATH2  = $(LIBPATH2) HPATH3  = $(LIBPATH3)
HPATH4  = $(LIBPATH4) HPATH5  = $(LIBPATH5) HPATH6  = $(SCRSPATH1)

PRINT   = lp -oc
TARDATE = ‘date +%d%m%y‘
TARFILE = wa$(TARDATE).tgz TAR = tar TARFLAGS= czvf TARTARGETS = *
```

```
FFLAGS  = -O3 -s CFLAGS  = -O3 -s -I$(HPATH1) -I$(HPATH2)
-I$(HPATH3)  -I$(HPATH4) -I$(HPATH5)  -I$(HPATH6)

CC  = cc -lm


geotop.exe:    $(OBJS) $(SRCS)
            $(CC) -o $(BINS) $(OBJS)

$(OBJS):    $(HDRS)     # Include comune a tutti i files

clean:;     @rm -f *.o core lint.out num print:;     @$(PRINT)
$(HDRS) $(SRCS) index:;     @ctags -wx $(HDRS) $(SRCS) lint:;
@lint $(SRCS) > lint.out num:;       @pr -n $(SRCS) > num ris:;
@cp $(SRCS) ./ris


tar:clean;  @if [ -f $(TARFILE) ]; then $(RM) $(RMFLAGS)
$(TARFILE); fi;
        @echo "creo il file $(TARFILE) ...";
        @ $(TAR) $(TARFLAGS) $(TARFILE) $(TARTARGETS)
```

Appendix B

Preprocessing programs

Before running **GEOTOP**, the user can run several postprocessing programs, to build input files. Here a brief explanation of the program **Sky view factor** is reported.

B.1 The Sky view factor

GEOTOP needs an input file with the sky view factor. The sky view factor is the angular fraction of sky visible from a point. Without obstructions, the factor is 1 and in a mountain environment the factor can be less than 0.6 and it can be important to take it in account for evaluating the diffuse solar radiation. The sky view factor is calculated separately with the program *Sky.c*(Verardo, 1998). Here is a brief description of the program.

Author and date: P. Verardo, 1998

Inputs:
1. File with elevation matrix;
2. File with convex point matrix (1 convex; 0 concave);
3. A resolution parameter n, the number of sectors in which the horizon is divided.

Returns:
1. File with sky view factor;

Needs: The program *Nabla2.c* to calculate the convex point matrix (conventional values). See the Horton (Rigon, 2001) manual for further details.

Sources: Sky.c, Nabla2.c

Appendix C

Postprocessing programs

After running **GEOTOP**, the user can run several postprocessing programs, to elaborate the output files. Here a brief explanation of the programs **clean_output6**, **postprocess** and **saturation** is reported.

C.1 clean_output6

This program needs as input only the output file **output6.txt** and writes the content in the file **output6.clean.txt** in a standard FluidTurtle format.

Author and date: G. Bertoldi, 2002

Inputs: 1. File output6.txt;

Returns: 1. File output6.clean.txt;

Needs: The program needs run before **GEOTOP**.

Sources: clean_output6.c

C.2 postprocess

This program elaborates several input and output files of **GEOTOP** and rewrites most results averaged on (1) time step basis (parameter **DT3**, see paragraph 7.1), (2) hourly basis, (3) daily basis, (4) the whole simulation.

Author and date: G. Bertoldi, 2002

Inputs: **Inpts** : File routing (postprocess.inpts);
input 1 : File GEOTOP Inpts (geo_top.inpts);
input 2 : File GEOTOP DTM;
input 3 : File GEOTOP Volume soil (Prova.Vol.txt);
input 4 : File GEOTOP Distance from channels (Prova.amp_mod.txt);

input 5 : File GEOTOP Meteo;
input 6 : File GEOTOP OUTPUT1;
input 7 : File GEOTOP OUTPUT2;
input 8 : File GEOTOP OUTPUT3;
input 9 : File GEOTOP OUTPUT4;
input 10 : File GEOTOP OUTPUT5;
input 11 : File GEOTOP OUTPUT6;
input 12 : File GEOTOP OUTPUT7.

Returns: **output 1** : File instantaneous data (outputdt.txt);
output 2 : File hourly data (outputhourly.txt);
output 3 : File daily data (outputday.txt);
output 4 : File total data (outputtot.txt).

Needs: The program needs to be run before **GEOTOP** and **clean_output6**.

Sources: postprocess.c

C.2.1 Example of Postprocess Inpts file

```
/** FILE POSTPROCESS.INPTS WITH I/0 FILES NAMES */

/** I/O FILES:
input1 FILE GEOTOP INPTS
input2 FILE GEOTOP DTM
input3 FILE GEOTOP VOLUME
input4 FILE GEOTOP DISTANCE2CHANNELS
input5 FILE GEOTOP METEO
input6 FILE GEOTOP OUTPUT1
input7 FILE GEOTOP OUTPUT2
input8 FILE GEOTOP OUTPUT3
input9 FILE GEOTOP OUTPUT4
input10 FILE GEOTOP OUTPUT5
input11 FILE GEOTOP OUTPUT6
input12 FILE GEOTOP OUTPUT7

output1 FILE INSTANT DATA
output2 FILE HOURLY DATA
output3 FILE DAILY DATA
output4 FILE TOTAL DATA */

index{1}
1:string array io files

{ geo_top.inpts, washita.200.dem.txt, Prova.Vol.txt,
Prova.amp_mod.txt, washita.meteo1997.27.6.txt, output1.txt,
output2.txt, output3.txt, output4.txt, output5.txt,
output6.clean.txt, output7.txt, outputdt.txt,
outputhourly.txt, outputday.txt, outputtot.txt, }
```

C.2.2 Example of Output dt file

```
    index{1}
    /** i t[h] jd aaaa mm  dd hh prec[m3/s] Et[m3/s] Qsub[m3/s]
    Qsup[m3/s] Q[m3/s] Qt[m3/s]  dV[m3/s]   prec[mm] Et[mm]
    Qt[mm] dV[mm] prec[mc_sum] Et[mc_sum] Qt[mc_sum] dV[mc_sum] sat[]
    sat_sur[] sat_sup[] sat_in[] Rn[W/m2] G[W/m2] H[W/m2] ET[W/m2]
    dE[W/m2] Ta[C] Ts[C] v[m/s] rh[%] Rsw[W/m2] */

    1:float matrix results{21601,36}
    ... data time step dt...
```

C.2.3 Example of Output day file

```
    index{1}
    /** i t[h] jd aaaa mm dd hh prec[m3/s] Et[m3/s] Qsub[m3/s]
    Qsup[m3/s] Q[m3/s] Qt[m3/s] dV[m3/s] prec[mm] Et[mm] Qt[mm]
    dV[mm] prec[mc_s] Et[mc_sum] Qt[mc_sum] dV[mc_sum] sat[]
    sat_sur[] sat_sup[] sat_in[] Rn[W/m2] G[W/m2] H[W/m2]
    ET[W/m2] dE[W/m2] Ta[C] Ts[C] v[m/s]  rh[%] Rsw[W/m2] */

    1:float matrix results{25,36}
    ... data time step 1 hour ...
```

C.2.4 Example of Output total file

```
    index{1}
    /** i t[h] jd aaaa mm  dd  hh prec[m3/s] Et[m3/s] Qsub[m3/s]
    Qsup[m3/s] Q[m3/s] Qt[m3/s] dV[m3/s] prec[mm] Et[mm] Qt[mm]
    dV[mm] prec[mc_sum] Et[mc_sum] Qt[mc_sum] dV[mc_sum] sat[]
    sat_sur[] sat_sup[] sat_in[] Rn[W/m2] G[W/m2] H[W/m2] ET[W/m2]
    dE[W/m2] Ta[C] Ts[C] v[m/s] rh[%] Rsw[W/m2]  */

1:float matrix results{1,36}
    ... data for the whole simulation ...

/** Some information about the simulation:
    matrix 140 rows 220 cols
    pixel tot   30800
    pixel val   14577
    pixel noval 16223
    volume      38419820.000000 m^3
    area        583080000.000000 m^2
    soil depht  0.065891 m
    elev max    475.799988  m
    elev min    323.100006  m
    elev med    391.712341  m
    dist2net    1206.043091   m
    pixel channel   1122
```

```
pixel hillslope 13455 */
```

C.3 saturation

This program calculates the saturation matrixes from the intermediate output files with the water content of each cell. The saturation is calculated using the equation 3.46.

Author and date: G. Bertoldi, 2002

Inputs: **Inpts** : File routing (saturation.inpts);

input 1 : File GEOTOP Inpts (geo_top.inpts);

input 2 : File with GEOTOP soil parameters (see par.7.6);

input 3 : File void volume GEOTOP Volume soil (Prova.Vol.txt in par. 8.8.1);

input 4 : File with GEOTOP final (or initial) water content (output3.txt in par. 8.3);

other inputs : Files with GEOTOP intermediate distributed results (see par. 8.8.2) with the name:

- **out07_NNN.txt** :with Vol_{sur}, water volume in the surface layer $[mm]$
- **out08_NNN.txt**: with Vol_{uns}, water volume in the unsatured upper layer $[mm]$;
- **out09_NNN.txt**: with Vol_{sat}, water volume in the lower satured layer $[mm]$.

These files are automatically read by the program.

Returns: **output 1** : File with final (or initial) saturation;

other outputs : Files with saturation during the simulation, with the name: **out14_NNN.txt**.

These files are automatically written by the program.

Needs: The program needs to be run before **GEOTOP**. All intermediate output files should exist.

Sources: saturation.c

C.3.1 Example of Saturation Inpts file

```
/** File saturation.inpts with I/0 files:
input1: geo_top.inpts
input2: file soil parameters
input3: file void volume
input3: file final (or initial) water content
output1: file final (or initial) saturation */

index{1}
1: string array io files{
geo_top.inpts, wahita.par.txt, Prova.vol.txt,
output3.txt, finalsat.txt }
```

Appendix D

GEOTOP GRASS interface

There are several scripts available to display graphically and elaborate several **GEOTOP** outputs, using the GRASS open source GIS program. We report here the related documentation for the scripts:

r.in.prova.geotop : import GEOTOP output files with the name "Prova.*" in to GRASS with a suitable color table.

r.in.out.geotop : import GEOTOP intermediate output files with the name "out**_***" in to GRASS.

d.color.multirast : gives the same color table to several raster files.

d.color.geotop : applies "d.color.multirast" to GEOTOP intermediate output files.

d.what.multirast : plot a GNUPLOT chart with the values of several raster maps in a selected point.

d.what.geotop : applies "d.what.multirast" to GEOTOP intermediate output files.

xganim.geotop : applies the GRASS command "xganim" to GEOTOP intermediate output files to play an animation.

r.out.mpeg.geotop : applies the GRASS command "r.out.mpeg" to GEOTOP intermediate output files to save an animation in a .mpeg file.

g.remove.geotop : removes all GEOTOP output raster from GRASS with the names "out**_***" and "Prova*".

D.1 r.in.prova.geotop

It import GEOTOP output files with the name "Prova.*" from FluidTurtle format to GRASS format using "ft2grass.geotop" (this executable have to be in the GEOTOP $WorkingPath); it imports all files in GRASS using the command "r.in.ascii", writes a appropriate color table for all rasters with a suitable color table.

Synopsis:

- r.in.prova.geotop -help
- r.in.prova.geotop $WorkingPath

Inputs:

$WorkingPath : the folder where are located the GEOTOP output files.

Other inputs : the program automatically searches and elaborates the following files:
Prova.Vol.txt, Prova.ca.txt, Prova.canopy_cover.txt, Prova.pond_volume.txt, Prova.Z0.txt, Prova.channelsixeldistance.txt, Prova.slopes.txt, Prova.albedo.txt, Prova.curv.txt,
Prova.soil_moisture.txt, Prova.amp_mod.txt, Prova.curv1.txt, Prova.drainage_direction.txt, Prova.top_ind.txt, Prova.area.txt, Prova.m.txt, Prova.vadose.txt, Prova.azimuth.txt, Prova.m_mod.txt, Prova.vegetazione.txt.

Returns:

GRASS raster maps : rasters have the same name, with no extensions:
Prova.Vol, Prova.ca, Prova.canopy_cover, Prova.pond_volume, Prova.Z0, Prova.channelsixeldistance, Prova.slopes, Prova.albedo, Prova.curv, Prova.soil_moisture, Prova.amp_mod, Prova.curv1, Prova.drainage_direction, Prova.top_ind, Prova.area, Prova.m, Prova.vadose, Prova.azimuth, Prova.m_mod, Prova.vegetazione.

Needs:

- the executable "ft2grass.geotop";
- GRASS have to be running.

Bugs: "ft2grass.geotop" have to be in the GEOTOP $WorkingPath directory.

Sources: bash script r.in.prova.geotop

Author and date: G. Bertoldi, 2002

D.2 r.in.out.geotop

It imports GEOTOP intermediate output files with the name "out**_***" from FluidTurtle format to GRASS format using "ft2grass.geotop" and imports all files into GRASS using the command "r.in.ascii".

Synopsis:

- r.in.out.geotop -help
- r.in.out.geotop $WorkingPath

Inputs:

$WorkingPath : the folder where the GEOTOP output files are located.

Other inputs : the program automatically searches all files with the names "out**_***.txt" in $WorkingPath.

Returns:

GRASS raster maps : rasters have the same name, without extensions: "out**_***".

Needs:

- the executable "ft2grass.geotop" have to be in the GEOTOP $WorkingPath directory;
- to have volumetric water content files (names "out14_***) one has to run first the program "saturation" (see par C.3);
- GRASS has to be running.

Bugs: "ft2grass.geotop" have to be in the GEOTOP $WorkingPath directory.

Sources: perl script r.in.out.geotop

Author and date: G. Bertoldi, 2002

D.3 d.color.multirast

It gives the same color table to several raster files. It calculates the minimum and the maximum value of all raster maps given as input and gives to all raster maps a color table with a range from minimum to maximum with the following rules:
blue (minimum) → green → yellow → red → violet (maximum).

Synopsis:

- d.color.multirast -help
- d.color.multirast raster_1 [raster_2] ... [raster_n]

Inputs: raster_1 [raster_2] ... [raster_n]: the raster maps list.

Returns:

- the color table for all raster maps
- the color rules file, saved in the GRASS database directory with the name "rules.tmp".

Needs: GRASS has to be running.

Bugs: the colortable is fixed and it is written in the script: to change colors one has to edit the script.

Sources: bash script d.color.multirast

Author and date: G. Bertoldi, 2002

D.4 d.color.geotop

Applies "d.color.multirast" to GEOTOP intermediate output files.

Synopsis:

- d.color.geotop -help
- d.color.geotop

Inputs: the program automatically searches all GRASS rasters with the names "out**_***".

Returns: the color table for all raster maps. For each file type (from 01 to 14) an only color table is choosen .

Needs:

- the output files should have been already imported by using "r.in.out.geotop".
- to elaborate the file types 14 you have to run first the program "saturation" (see par C.3);
- GRASS has to be running.

Bugs:

Sources: bash script d.color.geotop

Author and date: G. Bertoldi, 2002

D.5 d.what.multirast

It plot a GNUPLOT chart with the values of several raster maps in a selected point. It displays time evolution at user specific location raster files. The location of the point is selectet by the mouse in the active monitor.

Synopsis:

- d.what.multirast -help
- d.what.multirast d.what.multirast [-l ylabel] [-t title] [-f filename] [-e east] [-n north] [-b noplot] raster1 [raster2] [raster3] ... [rasterN]

Inputs: **raster1 [raster2] [raster3] ... [rasterN]**: the raster map to query.

Options:

-l ylabel : the label of the y axis (default "Y values").

-t title : the title of the plot (default "Values").

-f filename : with this option, the data are saved in the current directory in the file "filename.data" and the gnuplot script is saved in the file "filename.gnuplot".

-e east you can specify the east

-n north you can specify the north

-b noplot does not plot the output

Returns:

- a gnuplot graph with the plot of the rasters values;
- optionally the data in the file "filename.data" (written in the current directory)
- optionally the data in the file "filename.gnuplot" (written in the current directory).

Needs:

- The script requires gnuplot;
- GRASS has to be running.

Bugs:

Sources: bash script d.what.multirast

Author and date: G. Bertoldi, 2002

D.6 d.what.geotop

It applies "d.what.multirast" to GEOTOP intermediate output files, to plot the time series of output values in a selected point.

Synopsis:

- d.what.geotop -help
- d.what.geotop (interactive mode)
- d.what.geotop [parameters]

Inputs:

type : type of data to query (1 to 17, see example below D.6.1)

Returns:

- the gnuplot graph of the time series of the data type chosen in a user-selected location (see d.what.multirast).
- the data in the file "out**.data" (written in the current directory, where ** is the data type number, see D.6.1)
- the data in the file "out**.gnuplot" (written in the current directory).

Needs:

- the output files should have been already imported by using "r.in.out.geotop".
- to elaborate the file types 14 one has to run first the program "saturation" (see par C.3);

- GRASS have to be running.

Bugs:

- the non-interactive mode is not yet ready.
- it would be better for options 15, 16, 17 to plot a single four-line chart (we need to modify d.what.multirast).

Sources: bash script d.what.geotop

Author and date: G. Bertoldi, 2002

D.6.1 Example of d.what.geotop input window

```
============================================================
OPTION: Type of data to query
      key: type
required: YES
============================================================
 Single plots:
[ 1] R_n     net radiation [W/m^2]
[ 2] G       soil heat flux [W/m^2]
[ 3] H       sensible heat flux [W/m^2]
[ 4] Et      latent heat flux [W/m^2]
[ 5] dE/dt   energy storage in the canopy layer [W/m^2]
[ 6] Ts      surface soil temperature [C]
[ 7] Vol_sur water volume in the surface layer [mm]
[ 8] Vol_uns water volume in the unsatured upper layer [mm]
[ 9] Vol_sat water volume in the lower satured layer [mm]
[10] P_net   net precipitation [mm]
[11] W_t     canopy intercepted water [mm]
[12] Et_pm   latent heat flux, Penman-Monteith's equation [W/m^2]
[13] H_pm    sensible heat flux, Penman-Monteith's equation [W/m^2]
[14] sat     saturation (run before saturation program!) [ ]
------------------------------------------------------------
 Four windows plots:
[15] Energy Balance: 1) Rn,   2)G,       3)H(3),    4)ET
[16] Mass Balance:   1) Prec, 2)ET,      3)vol_sur, 4)sat
[17] Water Volumes:  1) sat,  2)vol_sur, 3)vol_uns, 4)vol_sat
============================================================
enter option [1-17] >
```

D.7 xganim.geotop

It applies the GRASS command "xganim" to GEOTOP intermediate output files to play an animation. Interactive display of GEOTOP output files animations, running xganim movie from GEOTOP distributed outputs.

Synopsis:

- xganim.geotop -help
- xganim.geotop (interactive mode)
- xganim.geotop [parameters]

Inputs:

type : type of data to query (1 to 17, see example above D.6.1)

Returns: the animation of the time series of the data type chosen (see GRASS command xganim).

Needs:

- the output files should have been already imported using "r.in.out.geotop".
- to have a homogeneous color table, it is better to run first "d.color.geotop".
- to elaborate the file types 14 one has to run first the program "saturation" (see par C.3);
- GRASS has to be running.

Bugs: the non-interactive mode is not yet ready.

Sources: bash script xganim.geotop

Author and date: G. Bertoldi, 2002

D.8 r.out.mpeg.geotop

It applies the GRASS command "r.out.mpeg" to GEOTOP intermediate output files, to save an animation in a .mpeg file. Interactive display of GEOTOP output files animations, creating a MPEG movie from GEOTOP distributed outputs.

Synopsis:

- r.out.mpeg.geotop -help
- r.out.mpeg.geotop (interactive mode)
- r.out.mpeg.geotop [parameters]

Inputs:

type : type of data to query (1 to 17, see example above D.6.1)

Options:

file : name of the output .mpeg file (default name gmovie**.mpeg, where ** is the data type code).

play : (y / n) asks to play the file with the program mpeg_play.

Returns: the .mpeg animation file of the time series of the data type chosen (see GRASS command r.out.mpeg).

Needs:

- the output files should have been already imported using "r.in.out.geotop".
- to have a homogeneous color table, it is better to run first "d.color.geotop".
- to elaborate the file types 14 one has to run first the program "saturation" (see par C.3);
- GRASS has to be running.
- it needs programs "mpeg_encode" and "mpeg_play".

Bugs:

- the non-interactive mode is not yet ready.
- the resolution of the .mpeg file is quite low.

Sources: bash script r.out.mpeg.geotop

Author and date: G. Bertoldi, 2002

D.9 g.remove.geotop

It removes all GEOTOP output raster with the names "out**_***" and "Prova*" from GRASS.

Synopsis:

- g.remove.geotop -help
- g.remove.geotop (interactive mode)

Options:

OK : (y / n) ask to remove files.

Needs:

- GRASS has to be running.

Bugs:

Sources: bash script g.remove.geotop

Author and date: G. Bertoldi, 2002

Appendix E

GEOTOP Gnuplot interface

There are several scripts available to graphic display **GEOTOP** outputs, using the Gnuplot open source GIS program. We report here the related documentation for the scripts:

plot.dt.geotop : plots instantaneous output data;

plot.day.geotop : plots daily output data;

plot.output5.geotop : plots output data for the control pixel.

E.1 plot.dt.geotop

It plots instantaneous output data from the file "outputdt.txt", obtained by the program "postprocess" (see par. C.2).

Synopsis:

- plot.dt.geotop -help
- plot.dt.geotop $WorkingPath

Inputs:

$WorkingPath : the folder where the GEOTOP output files are located.

Other inputs : the file "outputdt.txt", obtained by the program "postprocess" (see par. C.2).

Returns:

plots : it plots the following quantities:

1. Precipitation [mm]
2. Mass balance [m^3/s]: Flow, Flow Surface, Flow Subsurface, Evapotranspiration.
3. Mass balance [mm/dt]: Flow, Precipitation, Volume variation, Evapotranspiration.

4. Cumulative mass balance [m^3]: Flow, Precipitation, Water storage, Evapotranspiration.
5. Saturation []: Saturation, Sat surface, Sat upper, Sat lower.
6. Energy balance [W/m^2]: Rn, G, H, ET, dE/dt.
7. Surface temperature [C]: Ta, Ts.
8. Input data: Air temperature [C], Wind speed [m/s].
9. Input data: Relative humidity [$\%$], Shortwave radiation [W/m^2].

Files : the script creates the folder $WORKINGPATH/gnuplot, where the data in gnuplot format (file outputdt.gnuplot) and the gnuplot scripts (files: prec.dt.gnuplot, mass.mcs.dt.gnuplot, mass.mmd.dt.gnuplot, mass.sum.dt.gnuplot, en.dt.gnuplot, sat.dt.gnuplot, ts.dt.gnuplot, meteo1.dt.gnuplot, meteo2.dt.gnuplot) are stored.

Needs:

- the program requires gnuplot;
- to run before the program post-process.

Bugs:

Sources: bash script plot.dt.geotop

Author and date: G. Bertoldi, 2002

E.2 plot.day.geotop

It plots daily output data from the file "outputday.txt", obtained by the program "post-process" (see par. C.2).

Synopsis:

- plot.day.geotop -help
- plot.day.geotop $WorkingPath

Inputs:

$WorkingPath : the folder where the GEOTOP output filesare located .

Other inputs : the file "outputday.txt", obtained by the program "postprocess" (see par. C.2).

Returns:

plots : it plots the following quantities:

1. Precipitation [mm]
2. Mass balance [m^3/s]:Flow, Flow Surface, Flow Subsurface, Evapotranspiration.
3. Mass balance [mm/dd]:Flow, Precipitation, Volume variation, Evapotranspiration.
4. Cumulative mass balance [m^3]: Flow, Precipitation, Water storage, Evapotranspiration.

5. Saturation []: Saturation, Sat surface, Sat upper, Sat lower.
6. Energy balance [W/m^2]: Rn, G, H, ET, dE/dt.
7. Surface temperature [C]: Ta, Ts.
8. Input data: Air temperature [C], Wind speed [m/s].
9. Input data: Relative humidity [$\%$], Shortwave radiation [W/m^2].

Files : the script creates the folder $WORKINGPATH/gnuplot, where the data in gnuplot format (file outputday.gnuplot) and the gnuplot scripts (files: prec.day.gnuplot, mass.mcs.day.gnuplot, mass.mmd.day.gnuplot, mass.sum.day.gnuplot, en.day.gnuplot, sat.day.gnuplot, ts.day.gnuplot, meteo1.day.gnuplot, meteo2.day.gnuplot) are stored.

Needs:

- the program requires gnuplot;
- to run before the program postprocess.

Bugs:

Sources: bash script plot.day.geotop

Author and date: G. Bertoldi, 2002

E.3 plot.output5.geotop

It plots output data for the control pixel from the GEOTOP output file "output5.txt" (see par. 8.5).

Synopsis:

- plot.output5.geotop -help
- plot.output5.geotop $WorkingPath

Inputs:

$WorkingPath : the folder where the GEOTOP output files are located .

Other inputs : the GEOTOP output file "output5.txt" (see par. 8.5).

Returns:

plots : it plots the following quantities:

1. Input data: Air temperature [C], Wind speed [m/s].
2. Input data: Relative humidity [ ], Shortwave radiation [W/m^2].
3. Precipitation [mm]: prec, Net Prec.
4. Saturation []: Saturation.
5. Water volumes [m^3]: Vol surface, Vol upper, Vol lower.
6. Energy balance [W/m^2]: Rn, G, H, ET, dE/dt.
7. Surface temperatures [C]:temperatures of air (Ta), soil surface (Ts), first soil layer (T1), deepest soil layer (Tn).

8. Evaporation partition [m^3]: wet canopy evaporation (Evc), canopy transpiration (Etc), bare ground evaporation (Eg), total evapotranspiration (Et).

Files : the script creates the folder $WORKINGPATH/gnuplot, where the data in gnuplot format (file output5.gnuplot) and the gnuplot scripts (files: meteo1.output5.gnuplot, meteo2.output5.gnuplot, prec.output5.gnuplot, sat.output5.gnuplot, vol.output5.gnuplot, en.output5.gnuplot, ts.output5.gnuplot, et.output5.gnuplot) are stored.

Needs:

- the program requires gnuplot.

Bugs: The file ../gnuplot/output5.gnuplot contains also the following data: day, time, P, albedo, CDn, CHn, FM, FH, Rib, Wt, Et_PM, H_PM, r_c, ro_s, c_s, k_s. If you want to plot these data you can create other gnuplot scripts.

Sources: bash script plot.output5.geotop

Author and date: G. Bertoldi, 2002

Bibliography

[1] Andrè, J C., et al. . Evaporation over land-surfaces, first results from hapex-mobilhy special observing period. *Annales Geophysicae*, 6:477–492, 1988.

[2] Arnfield A. J. Evaluation of empirical expressions for the estimation of hourly and daily totals of atmospheric longwave emission under all sky conditions. *Quart. J. Roy. Meteorol. Soc.*, 105:1041–1052, 1979.

[3] Bathurst, J. C. *Flow resistence through the channel network* in *Channel Networks Hydrology*. Edited by K. Beven and M. J. Kirkby. John Wiley, 1993.

[4] Bertoldi, G., Rigon, R., Over, T. M. Un indagine sugli effetti della topografia con il modello geotop. *Atti del XVIII Convegno Nazionale di Idraulica e Costruzioni Idrauliche*, 1:313–324, September 16 - 19 2002.

[5] Best M. J. A model to predict suface temperatures. *Bound. Layer Meteor.*, 88(2):279–306, 1998.

[6] Beven, K. J. *Rainfall-runoff modelling: the primer*. Wiley, 2000.

[7] Beven K.J., Kirkby, M. J. A phisically based variable contributing area model of basin hydrology. *Hydrol. Sci. Bull.*, 24(1):43–49, 1979.

[8] Bolton D. The computation of equivalent potential temperature. *Mon. Wea. Rew.*, 108:1046–1099, 1980.

[9] Bolz H. M. Die abhängigkeit der infraroten gegenstrahlung von der bewölkerung. *Zeitung Metereol.*, (3):201–203, 1949.

[10] Brutsaert W. On a derivable formula for long-wave radiation from clear skies. *Water Resources Research*, 11(5):742–744, October 1975.

[11] Brutsaert W. *Evaporation into the Atmosphere: Theory, Hystory and Applications*. Kluver Academic Publisher, 1982.

[12] Castelli F., Entekhabi D., Caporali E. Estimation of surface heat flux and an index of soil moisture using adjoint-state energy balance. *Water Resources Research*, 35(10):3115–3125, 1999.

[13] Ciarapica L. *Un modello afflussi-deflussi distribuito applicabile dalla scala di versante alla scala*. Ph.d. thesis, Bologna, 1998. E. Todini supervisor.

[14] Clapp R. B., Hornberger G. M. Empirical equations for some hydraulic properties. *Water Resources Research*, 14:601–605, 1978.

[15] Cozzini A. *Sulla deduzione dei processi geomorofologici a partire dai modelli digitali del terreno*. Master thesis, Corso di laurea in Ingegneria per L'Ambiente e il Territorio, 2000.

[16] Crago R. D. *Daytime evaporation from conservation of surface flux ratios* in *Scaling up in Hydrology using Remote Sensing*. Edited by Stewart J.B. et al. Wiley, 1996.

[17] Daamen C. C. and Simmonds, L. P. Measurement of evaporation from bare soil and its estimation using surface resistance. *Water Resources Research*, 32(5):1393–1402, 1996.

[18] Daamen C. C. and Simmonds L. P. Soil, water, energy and transpiration, a numerical model of water and energy fluxes in soil profiles and sparse canopies. Technichal report, University of Reading, 1997.

[19] Daamen C. C., Pearson, Gurney, Simmonds L. P. Combined modelling of shortwave and thermal radiation for one-dimensional svats. *Hydrology and Earth System Sciences*, 3(1):15–30, 1999.

[20] de Franceschi M. *Misure di flussi turbolenti nello strato limite atmosferico mediante anemometro sonico*. Master thesis, Corso di laurea in Ingegneria per L'Ambiente e il Territorio, 1999.

[21] Deardorff J. W. Efficient prediction of ground surface temperature and moisture with inclusion of a layer of vegetation. *Journal of Geophisical Research*, 83(C4):1889–1903, April 1978.

[22] Dickinson R. E. Modelling evapotranspiration for three-dimensional global climate models, climate processes and climate sensitivity. *Geophisical Monograph, Maurice Erving*, 5:58–72, 1984.

[23] Kennedy P.J. Dickinson R.E., Heanderson-Sellers A. and M. Wilson. Biosphere atmosphere transfer scheme (bats) for the ncar community climate model. Technical Note NCAR/TN-275+STR, NCAR, 1986.

[24] Dietrich W. E. et al. Analysis of erosion thresholds, channel networks, and landscape morphology using a digital terrain model. *The Journal of Geology*, 101(2):259–278, March 1993.

[25] Dietrich W. E., Reiss Robert et al. A process-based model for colluvial soil depth and shallow landsliding using digital elevation data. *Hydrological processes*, 9:383–400, 1995.

[26] Dingman L. S. *Phisical Hydrology*. Prentice Hall, 1994.

[27] Eagleson P. S. *Dynamic Hydrology*. McGraw-Hill, 1970.

[28] Fairfield J. and Leymarie P. Drainage networks from grid digital elevation models. *Water Resources Research*, 30(6):1681–1692, 1991.

[29] Fleichinger et al. Modelling evapotranspiration and surface energy budgets across a watershed. *Water Resources Research*, 32(8):2539–2548, 1996.

[30] Franchini M., Wendling M. J., Obled C., Todini E. Phisical interpretation and sensitivity analysis of the topmodel. *Journal of Hydrology*, 175:293–338, 1996.

[31] Frohlich C, Brusa R. W. Solar radiation and its variation in time. *Solar Pyisic*, 74:209–215, 1981.

[32] Garrat J. R. *The Atmospheric Boundary Layer*. Cambridge University Press, 1992.

[33] Grayson, R. B., Moore, I.D. and Boschl, G. Distribute parameter hydrologic modelling using vector elevation data: Thales and tapes-c. In *Computer Models of Watershed Hydrology, Singh ed.*, Water Resources Publications, pages pp. 21–29, Highlands Ranch, CO, 1995.

[34] Heimsath Arjun M., Dietrich William E. The soil production function and landscape equilibrium. *Nature*, 388:358–361, 1997.

[35] Henderson-Sellers, Pitman A. J., Love P.K., Irannejad P. and Chen T.H. The project for intercomparision of land surface parameterisation schemes (pilps): phases 2 and 3. *Bulletin of the American Meteorological Society*, (76):489–503, 1995.

[36] Henderson-Sellers, Yang Z.L., Dickinson R.E. The project for intercomparison of land-surface parameterization schemes. *Bull. of the Amer. Met. Soc.*, 74:1335–1349, 1993.

[37] Idso et al. Net radiation - soil heat flux relations as influenced by soil water content variations. *Bound. Layer Meteor.*, (9):113–135, 1975.

[38] Incropera F. P. and DeWitt D.P. *Fundamentals of Heat Transfer*. Third Edition. John Wiley and Sons, New York, 1990.

[39] Iqbal M. *An Introduction to Solar Radiation*. Academic Press, 1983.

[40] Jansson, P. E. Soil model. Technichal report, University of Uppsala, 1997.

[41] Kasten F., Czeplak G. Solar and terrestral radiation dependent on the amount and type of cloud. *Solar Energy*, 24:177–89, 1980.

[42] Katul G. G., Parlange M. B. A penman-brutsaert model for wet surface evaporation. *Water Resources Research*, 28(1):121–126, January 1992.

[43] Kitanidis P. K. *Introduction to Geostatistic Application in Hydrogeology*. Cambridge Univ. Press, 1997.

[44] Kondratyev. *Radiation in the atmosphere*. Academic Press, 1969.

[45] Kot See Chun, Song Yu. An imporovement of the louis scheme for the surface layer in an atmospheric modelling system. *Bound. Layer Meteorol.*, 88(2):239–254, 1998.

[46] Liang X., Lettenmaier P., Wood E. F., Burges S. J. . A simple hydrologically based model of land surface water and energy fluxes for general circulation models. *Journal of Geophisical Research*, 99(D7):14415–14428, July 1994.

[47] Louis J. F. A parametric model of vertical eddy fluxes in the atmosphere. *Bound. Layer Meteor.*, (17):187–202, 1979.

[48] Manabe S. Climate and ocean circulation. *Mon. Wea. Rew.*, 17:187–202, 1969.

[49] Manabe, S. Climate and ocean circulation. i. the atmospheric circulation and the hydrology of the earth's surface. *Monthly Weather Review*, (97):739–774, 1969.

[50] Marani M., Rigon R., (edited by). *Hydromteorology and Climatology*. Istituto Veneto di Scienze, Lettere de Arti, 1997.

[51] Marth L. and Pan H. A two-layer model of soil hydrology. *Boundary Layer Meteorology*, (23):1–20, 1984.

[52] Mengelkamp H.T., Warrach K., Raschke E. Sewab - a parametrization of the surface energy and water balance for atmospheric and hydrologic models. *Advances in Water Resurces*, 23:165–175, October 1999.

[53] Mitchell, K., Lin Y., Rogers E., Marshall C., Ek m., Lohmann D., Schaake J., Tarpley D., Grunmann P., Maninkin G., Duan Q e Koren V. Recent gcip-sponsored advancements in coupled land-surface modelling and data assimilation in the ncep eta mesoscale model. 15th conference on hydrology, AMS, Long Beach, CA, 9-14 January 2000.

[54] Nascimbeni M. *Modelli chimici e idrodinamici per i piccoli laghi*. Master thesis, Corso di laurea in Ingegneria per L'Ambiente e il Territorio, 1999.

[55] Noilhan J.,Planton S. A simple parametriztion of land surface processes for meteorological models. *Mon. Wea. Rev*, (117):536–585, 1989.

[56] Paci Marco. *Ecologia Forestale*. Edizioni Agricole, 1996.

[57] Paltrige G.W., Platt C.M.R. *Radiative Processes in Meteorology and Climatology*. Elsevier, 1976.

[58] Parlange M. B., Eichinger W. E., Albertson J. D. . Regional scale evaporation adn the atmospheric boundary layer. *Reviews of Geophisic*, 33(1):99–124, 1995.

[59] Pegoretti M. *Geomodel: implementazione di un modello scalabile di deflusso e bilancio idrologico di bacino*. Master thesis, Corso di laurea in Ingegneria per L'Ambiente e il Territorio, 1999.

[60] Pielke. *Mesoscale Meteorological Modeling*. Academic Press, 1984.

[61] Prosser I. P. and Abernethy B. Predicting the topographic limit to a gully network using a digital terrain model and process thresholds. *Water Resour. Res*, 32(7):2289–2298, 1996.

[62] Rigon R. Appunti di idrologia. Technichal report, University of Trento, 2000.

[63] Rigon R. The fluidtutle manual. 2002.

[64] Rigon R. , Cozzini A. Horton: un insieme di programmi open source per la analisi geomorfologica quantitativa dei bacini montani. Internal report, University of Trento, 2001.

[65] Rigon, R., Bertoldi, G., Over, T. M. Geotop: un modello del ciclo idrologico. *Atti del XVIII Convegno Nazionale di Idraulica e Costruzioni Idrauliche*, 1:303–312, September 16 - 19 2002.

[66] Rinaldo A., Marani A. e Rigon R. Geomorphological dispersion. *Water Resour. Res.*, 27(4):513–525, 1991.

[67] Rinaldo A., Marani A., Rigon R. Geomorphological dispersion. *Water Resources Research*, 27(4):513–525, 1991.

[68] Rinaldo et al. Self-organized fractal river networks. *Phys. Resour. Research*, 1994.

[69] Rodriguez-Iturbe, I. and Rinaldo, A. *Fractal River Basins*. Cambridge University Press, 1997.

[70] Rodriguez-Iturbe, I. and Valdes. The geomorphic structure of the hydrologic response. *Water Resour Res.*, 18(4), 1979.

[71] Rodriguez-Iturbe I. e Rinaldo A. *Fractal river basins*. Cambridge University Press, 1997.

[72] Salvaterra M. *Applicazione di un modello di bilancio idrologico al bacino del Lago di Serraia (TN)*. Diploma thesis, Corso di diploma in Ingegneria per L'Ambiente e il Territorio, 2000.

[73] Sellers P. et al. A simple biosphere model (sib) for use within general circulation models. *Journal of Atmospheric Science*, 73:305–310, 1986.

[74] Sellers, P.J., et al. An overview of the fife experiment. *Journal of Geophyiscal Research*, (17):18345–18373, 1997.

[75] Sellers, P.J., Mintz Y., Sus Y.C. and Calcher A. A simple biosphere model (sib) for use within general circulation models. *Journal of the Atmospheric Sciences*, 43(6):505–531, 1986.

[76] Sellers, W. D. *Phisical Climatology*. Univ. of Chicago Press, 1965.

[77] Spencer J. W. Fourier series representation of the position of the sun. *Search*, 2(5):172, 1971.

[78] Stockler, R. Sull'utilizzo delle mappe digitali del terreno nello studio della risposta idrologica. Master thesis, Padova, 1998. A. Rinaldo supervisor.

[79] Stull R. B. *An itroduction to Boundary Layer Meteorology*. Kluver Academic Publisher, 1988.

[80] Tarboton, D. G., T. G. Chowdhury and T. H. Jackson. A spatially distributed energy balance snowmelt model. proceedings of a boulder symposium, ed. k. a. tonnessen et al. *Biogeochemistry of Seasonally Snow-Covered Catchments, IAHS Publ.*, 108(228):141–155, July 3-14 1995.

[81] Verardo P. *L'evapotraspirazione nei bacini montani: modellazione numerica ed applicazione ad un caso di studio*. Master thesis, Corso di laurea in Ingegneria per L'Ambiente e il Territorio, 1998.

[82] Webb E. K. *Evaporation from catchments* in *Prediction in Catchment hydrology*. Edited by Chapman T. G., Dunin F. X. Australian Academy of Science, 1975.

[83] Western, A. W., Grayson R. B. and T.R. Green. The tarrawarra data set: soil moisture patterns, soil characteristics and hydrological flux measurements. *Water Resour. Res.*, 34(10):2765–2768, 1998.

[84] Wood, E. F., D. P. Lettenmaier, and V.G. Zartarian. A land surface hydrology parametrization with subgrid variability for general circulation models. *Journal of Geophysical Research*, D3(97):2717–2728, 1992.

[85] R.A. Woods. Marvex: Identifying the causes of saptially-variabile hydrology. In *Proceedings of the 24th Hydrology and Water Resources Symposium*, number 551, Auckland, November 1997.